# A new perspective on the simulation of cross-correlated random fields

Hongzhe Dai[a,] *, Ruijing Zhang[a] and Michael Beer[b,c,d]

[a]*School of Civil Engineering, Harbin Institute of Technology, Harbin 150090, China*

[b]*Institute for Risk and Reliability, Leibniz Universität Hannover, Callinstr. 34, Hannover, Germany*

[c]*Institute for Risk and Uncertainty and School of Engineering, University of Liverpool, Peach Street, Liverpool L69 7ZF, UK*

[d]*International Joint Research Center for Engineering Reliability and Stochastic Mechanics, Tongji University, 1239 Siping Road, Shanghai 200092, PR China*

(*Corresponding Author: Hongzhe Dai, E-mail: hzdai@hit.edu.cn)

---

**Abstract:** Cross-correlated random fields are widely used to model multiple uncertain parameters and/or phenomena with inherent spatial/temporal variability in numerous engineering systems. The effective representation of such fields is therefore the key element in the stochastic simulation, reliability analysis and safety assessment of engineering problems with mutual correlations. However, the simulation of such fields is generally not straightforward given the complexity of correlation structure. In this paper, we develop a unified framework for simulating non-Gaussian and non-stationary cross-correlated random fields that have been specified by their correlation structure and marginal cumulative distribution functions. Our method firstly represents the cross-correlated random fields by means of a new general stochastic expansion, in which the fields are expanded in terms of a set of deterministic functions with corresponding random variables. A finite element discretization scheme is then developed to further approximate the fields, so that the sets of deterministic functions reflecting the cross-covariance structure can be straightforwardly determined from the spectral decomposition of the resulting discretized fields. For non-Gaussian random fields, an iterative mapping procedure is developed to generate random variables to fit non-Gaussian marginal distribution of the fields. By virtue of the remarkable property of the presented stochastic expansion, i.e., various random fields share an identical set of random variables, the framework we develop is conceptually simple for simulating non-Gaussian cross-correlated fields with arbitrary covariance functions, which need not be stationary. In particular, the developed method is further generalized to a consistent framework for the simulation of multi-dimensional random fields. Five illustrative examples, including a spatially varying non-Gaussian and nonstationary seismic ground motions, are used to demonstrate the application of the developed method.

*Keywords*: Cross-correlation; Random field simulation; Finite element discretization; Dimension reduction; Non-Gaussian.

---

## 1. Introduction

In the numerical modeling of many engineering applications, the uncertainties of the propagating media may significantly influence the stochastic solution and reliability analysis of structural systems [1-4]. This led the scientific community to recognize the importance of a probabilistic approach to engineering problems. In a probabilistic treatment of uncertainties in analyzing and designing physical systems, the use of random fields gained momentum due to the continued increase in available computational resources and nowadays is commonly used in multidisciplinary fields [5-9]. For instance, many real-life problems of interest, such as earthquake ground motions, fluid-structure interaction, acoustic propagation, multi-scale modeling of materials, to mention a few, involve multiple uncertain parameters and/or phenomena with inherent spatial variability. This type of uncertainty should be modeled and synthesized by means of random fields with mutual correlations, known as cross-correlated random fields [10-12]. The stochastic response and subsequent safety assessment of these engineering problems are often

obtained though simulation-based approaches, which are the most commonly used among the procedures available in the literature. Since the crux of the simulation-based techniques is the ability to accurately generate realizations of the random fields that possess the desired probability law to a reasonable degree, it is of fundamental importance to develop appropriate mathematical frameworks to model and simulate cross-correlated random fields effectively [1,13].

Over the years various approaches have been developed for the simulation of non-Gaussian and non-stationary cross-correlated random fields with specified non-Gaussian marginal distributions and second-order correlations, i.e., correlation functions or evolutionary power spectral density (PSD) functions. A first class of approach is the spectral representation method (SRM), which was originally developed for the simulation of Gaussian scalar fields. Since there is no theoretical obstacle for the extension of simulation of scalar fields to that of cross-correlated Gaussian fields [14], the SRM has been generalized to the simulation of non-Gaussian non-stationary cross-correlated fields by further using the translation process theory [15]. In particular, SRM has been successfully applied for modelling phenomena with inherent spatial variability in real-life problems of interest, e.g. wind velocity, earthquake ground motions, etc [11,16,17]. Another class of method is based on Karhunen-Loeve (KL) expansion, which was also initially utilized for simulating Gaussian scalar fields [17]. Phoon et al. extended the KL expansion to simulate non-Gaussian scalar fields by iteratively updating the distribution of the underlying non-Gaussian K-L random variables [19,20]. However, the most significant challenge to generalize the method for simulating cross-correlated fields is that the KL expansion cannot expand the cross-correlated fields into consistent expansions in a straightforward manner, and one has to assume that the cross-correlated fields share the same auto-correlation structure and that the cross-correlation structure can be simplified as a cross-correlation coefficient, such as those by Vořechovský [21]. Although such assumptions facilitate the eigen-decomposition of the correlation structure, undesired spurious cross-correlation may arise among cross-correlated random fields. In order to obviate these limitations, the cross-correlation structure was further represented in terms of correlated random variables in [22]. Nevertheless, the extension of the method to non-Gaussian fields is not straightforward. For this line of approach to be successful in practice, it is crucial to have a general-purpose and highly effective scheme for the simulation of cross-correlated random fields with arbitrary correlation structures.

The goal of the present paper is to develop a conceptually simple methodology for the simulation of non-Gaussian and non-stationary cross-correlated random fields with arbitrary correlation structures and marginal distributions. In order to circumvent the difficulties in representing correlation structures encountered in KL expansion, a general stochastic expansion scheme is firstly presented to represent the cross-correlated random fields, in which the fields are expanded in terms of a complete set of deterministic basis functions with corresponding random coefficients. By virtue of a significant property of the presented expansion, i.e., multiple random fields can be expanded under an identical set of random variables, both auto-covariances and cross-covariances among all components of the fields can be simultaneously reflected. A finite element discretization scheme is subsequently developed to further approximate the fields, so that the spectral decomposition might be readily utilized on the resulting discretized covariance matrix of the fields. By further coupling with a dimension reduction technique, the sets of deterministic functions associated with each component of the fields, together with the optimal number of these functions, can be straightforwardly determined. For Gaussian cross-correlated field, uncorrelated random coefficients are Gaussian and thereby can be completely determined by the first two order statistics. However, such simplification does not exist in general non-Gaussian fields. For non-Gaussian cross-correlated fields, an iterative mapping procedure is developed to fit the non-Gaussian marginal distribution of all components. In this manner, the target fields can be synthesized on the basis of the set of obtained deterministic functions and the corresponding random variables. The developed methodology thereby offers a unified framework for simulating non-Gaussian cross-correlated random fields with arbitrary covariance functions, which need not be stationary. In addition, the

developed methodology is further generalized to a consistent framework for the simulation of multi-dimensional random fields.

The rest of this paper is organized as follows: the present non-Gaussian KL expansion for scalar non-Gaussian fields is firstly introduced in Section 2. The developed methodology for simulating non-Gaussian and non-stationary cross-correlated random fields is described in Section 3, followed by the extension of the method for the simulation of multi-dimensional random fields in Section 4. Five illustrative examples are finally given in Section 5 to demonstrate the application of the developed method.

## 2. Non-Gaussian Karhunen-Loève expansion for scalar random fields

The KL expansion is a series expansion method for the representation of the random fields [23,24]. The expansion is based on a spectral decomposition of the covariance function of the field [1]. It states that a second-order field $w(x)$, which is indexed on a bounded domain $\mathcal{D}$, can be approximated by the following truncated KL series

$$\hat{w}(x) = \overline{w}(x) + \sum_{n=1}^{M} \sqrt{\lambda_n}\, f_n(x)\, \xi_n \tag{1}$$

where $\overline{w}(x)$ is the mean function of the field, $M$ is the number of terms of KL series, $\{\xi_n\}$ is a set of uncorrelated random variables with zero mean and unit variance given by

$$\xi_n = \frac{1}{\sqrt{\lambda_n}} \int_D \left[ w(x) - \overline{w}(x) \right] f_n(x)\, dx \tag{2}$$

$\lambda_n$ and $f_n(x)$ are the eigenvalues and eigenfunctions of the covariance function $C(x_1, x_2)$ of the field, obtained from solving the following homogeneous Fredholm integral equation of the second kind:

$$\int_{\mathcal{D}} C(x_1, x_2)\, f_n(x_1) dx_1 = \lambda_n f_n(x_2) \tag{3}$$

the solution of which can be determined numerically for problems of practical interests [25]. It is known that, for fixed $M$, the resulting random field approximation $\hat{w}(x)$ is optimal among series expansion methods with respect to the global mean square error [1].

If the field $w(x)$ is Gaussian, then $\{\xi_n\}$ are independent standard Gaussian random variables. But for non-Gaussian field, $\{\xi_n\}$ are generally non-Gaussian and, in order to determine their distributions, Eq.(2) must be solved. The integrand in Eq.(2) is obviously unknown thus requiring iterative method to compute these unknown KL distributions. The most used iteration algorithm, which has been proven effective in many applications, is briefly summarized as follows. Details can be found in [19,20].

**Step 1:** Generate $N$ sample functions of the non-Gaussian field using the truncated KL expansion as

$$\hat{w}(x, \theta_m) = \overline{w}(x) + \sum_{n=1}^{M} \sqrt{\lambda_n}\, f_n(x)\, \xi_n^{(k)}(\theta_m), \quad m = 1, \cdots, N \tag{4}$$

where $k$ is the iteration number and $m$ is the sample number, and then estimate the simulated covariance and marginal CDF as

$$\hat{C}^{(k)}(x_1, x_2) = \frac{1}{N} \sum_{m=1}^{N} \left[ \hat{w}^{(k)}(x_1, \theta_m) - \hat{w}(x_1) \right] \left[ \hat{w}^{(k)}(x_2, \theta_m) - \hat{w}(x_2) \right] \tag{5}$$

and

$$\hat{F}^{(k)}(y / x) = \frac{1}{N} \sum_{m=1}^{N} \mathbb{I}\left[ \hat{w}^{(k)}(x, \theta_m) \le y \right] \tag{6}$$

where $y$ indicates the value of the empirical distribution function for a non-Gaussian realization, and $\mathbb{I}(A)$ is the

indicator function for event $A$, having the value 1 if event $A$ occurs and the value 0 otherwise. The simulated marginal CDF $\hat{F}(\cdot / x)$, which is the probability distribution of $\hat{w}(x)$ evaluated at a specific point $x$, does not necessarily agree with the target marginal CDF.

**Step 2:** Transform each sample function to match the target marginal cumulative distribution $F$

$$\eta^{(k)}(x,\theta_m) = F^{-1}\hat{F}^{(k)}\left[\hat{w}^{(k)}(x,\theta_m)\right], \quad m = 1,\cdots,N \tag{7}$$

and update the next generation of random variables $\xi_n^{(k+1)}(\theta)$ as

$$\xi_n^{(k+1)}(\theta_m) = \frac{1}{\sqrt{\lambda_n}}\int_D\left[\eta^{(k)}(x,\theta_m) - \overline{\eta}^{(k)}(x)\right] f_n(x)\,dx \tag{8}$$

where $\overline{\eta}^{(k)}(x)$ is the mean of $\eta^{(k)}(x,\theta)$. Since $\xi_n^{(k+1)}(\theta)$ is a zero mean vector by virtue of Eq.(8), one needs to standardize $\xi_n^{(k+1)}(\theta)$ to unit variance [19]. In [20], a Latin hypercube orthogonalization technique was further employed to reduce the product-moment correlations between $\xi_n^{(k+1)}(\theta)$.

**Step 3:** Repeat step 1 and 2 until the sample functions of the field achieved the target marginal CDF.

In the non-Gaussian KL expansion algorithm, the target covariance function is maintained, while the probability distributions of KL random variables are updated iteratively. It has been shown that good results can be achieved when simulating highly skewed non-Gaussian random fields with the method [20].

## 3. Simulation of non-Gaussian and non-stationary cross-correlated random fields

Consider a cross-correlated random fields $\boldsymbol{\omega}(\mathbf{x})$ with a set of components $\omega_i(x_i), i = 1,2,\cdots,n$, the auto/cross correlation structures between the fields $\boldsymbol{\omega}(\mathbf{x}) = \{\omega_1(x_1),\cdots,\omega_n(x_n)\}$ are defined by its $n(n+1)/2$ covariance functions

$$C_{ij}(x_i,x_j) = \mathbb{E}\left[\omega_i(x_i)\omega_j(x_j)\right], \quad i,j = 1,2,\cdots,n \tag{9}$$

where quantity $C_{ii}(x_{i1},x_{i2})$ in Eq.(9) is the auto-covariance of field $\omega_i(x_i)$. It is known that, if components of $\boldsymbol{\omega}(\mathbf{x})$ are mutually independent, the KL expansion can be readily applied, leading to multiple series which can be constructed separately, i.e.,

$$\omega_i(x_i) = \sum_{j=1}^{\infty}\sqrt{\lambda_{ij}}\,f_{ij}(x_i)\,\xi_{ij} \tag{10}$$

where $\xi_{ij}$ are uncorrelated random variables with zero means and unit variances, and $\lambda_{ij}$ and $f_{ij}(x)$ are the eigenvalues and eigenfunctions of the covariance function $C_{ii}(x_1,x_2)$ of component $\omega_i(x_i)$, respectively, obtained from solving homogenous Fredholm integral equation. The eigenfunctions $f_{ij}(x)$ form a complete orthogonal set of basis functions for the random field $\omega_i(x_i)$. The importance of KL expansion stems from its optimality in the sense that, it minimizes the total mean-square error. The reduction of a number of expansion terms from such a truncation has a significant impact on the computational demand for probabilistic investigations. Despite its theoretical importance, the KL expansion works only for a random field or ensembles of statistically independent random fields. Its generalization to cross-correlated random fields is not straightforward because practical difficulties arise in the representation of correlation structures of the fields due to its bi-orthogonal property. The inherent reason is that the sets of variables $\{\xi_{ij}\}$ and $\{\xi_{kj}\}$ are statistically independent when $i \neq k$, and hence the autocorrelation as well as the cross-covariances can not be simultaneously reflected. In this context, new stochastic expansion scheme needs to be developed to circumvent the difficulties in simultaneously representing the *auto-* and *cross-correlation* of the fields.

### 3.1. General stochastic expansion of cross-correlated random fields

For a zero mean random field $\omega(x)$, we construct a new stochastic expansion under general form

$$\omega(x)=\sum_{i=1}^{\infty} g_i(x)\eta_i \tag{11}$$

where $g_i(x)=\mathbb{E}\left[\omega(x)\eta_i\right]$, and $\{g_i(x)\}$ are a set of complete deterministic functions, and $\eta_i$ are a set of uncorrelated random variables with mean and covariance function given by

$$\mathbb{E}[\eta_i]=0,\quad \mathbb{E}\left[\eta_i\eta_j\right]=\delta_{ij} \tag{12}$$

where $\delta_{ij}$ is the Kronecker-delta function. Note that the set of deterministic functions $g_i(x)$ are not orthogonal nor normalized. Unlike the KL expansion, the representation of $\omega(x)$ in the context of the presented stochastic expansion is not unique because there is no orthogonal constraint imposed on the set of deterministic functions $g_i(x)$ in Eq.(11). This distinctive property makes it possible to represent multiple random fields in terms of an identical set of uncorrelated random variables, which will be quite preferable in the simulation of cross-correlated random fields. As a direct consequence of the presented stochastic expansion, covariance function $C(x_1,x_2)$ of the field $\omega(x)$ yields

$$\begin{aligned} C(x_1,x_2)&=\mathbb{E}\left[\sum_{i=1}^{\infty} g_i(x_1)\eta_i\sum_{j=1}^{\infty} g_j(x_2)\eta_j\right]\\ &=\sum_{i=1}^{\infty}\sum_{j=1}^{\infty} g_i(x_1)g_j(x_2)\mathbb{E}\left[\eta_i\eta_j\right]=\sum_{i=1}^{\infty} g_i(x_1)g_i(x_2)\end{aligned} \tag{13}$$

For practical implementation, the representation of $\omega(x)$ can be obtained by truncating the presented expansion in Eq.(11) at the *M*-th term:

$$\hat{\omega}(x)=\sum_{i=1}^{M} g_i(x)\eta_i \tag{14}$$

and the covariance function corresponding to the truncated series are

$$\hat{C}(x_1,x_2)=\sum_{i=1}^{M} g_i(x_1)g_i(x_2) \tag{15}$$

We note that the convergence of the truncated expansion in Eq.(14) has to be affirmed so that the general stochastic expansion could be a rational candidate in practice. The prove of the convergence can be found in Appendix.

By means of the presented general stochastic expansion, each component of the cross-correlated random field $\boldsymbol{\omega}(\mathbf{x})$ is approximated by

$$\omega_i(x_i)=\sum_{j=1}^{\infty} g_{ij}(x_i)\eta_j,(i=1,...,n) \tag{16}$$

with the resulting auto-covariance functions and cross-correlation functions given by

$$\begin{aligned} C_{ii}(x_{i1},x_{i2})&=\mathbb{E}\left[\omega_i(x_{i1})\omega_i(x_{i2})\right]\\ &=\mathbb{E}\left[\sum_{j=1}^{\infty} g_{ij}(x_{i1})\eta_j\sum_{k=1}^{\infty} g_{ik}(x_{i2})\eta_k\right]\\ &=\sum_{j=1}^{\infty} g_{ij}(x_{i1})g_{ij}(x_{i2})\end{aligned} \tag{17}$$

and

$$
\begin{aligned}
C_{ij}\left(x_i, x_j\right) &= \mathbb{E}\left[\omega_i\left(x_i\right)\omega_j\left(x_j\right)\right] \\
&= \mathbb{E}\left[\sum_{k=1}^{\infty} g_{ik}\left(x_i\right)\eta_k \sum_{l=1}^{\infty} g_{jl}\left(x_j\right)\eta_l\right] \\
&= \sum_{k=1}^{\infty} g_{ik}\left(x_i\right) g_{jk}\left(x_j\right)
\end{aligned} \tag{18}
$$

As a direct consequence of Eq.(17), the auto-correlation structures of components of a cross-correlated field can be different from each other, thus the assumption that cross-correlated fields has to share the same auto-correlation structure in [21] is no longer needed. Correspondingly, truncated versions of such representations have the form

$$
\hat{\omega}_i\left(x_i\right) = \sum_{j=1}^{N} g_{ij}\left(x_i\right)\eta_j, \left(i = 1, ..., n\right) \tag{19}
$$

$$
\hat{C}_{ii}\left(x_{i1}, x_{i2}\right) = \sum_{j=1}^{N} g_{ij}\left(x_{i1}\right) g_{ij}\left(x_{i2}\right) \tag{20}
$$

$$
\hat{C}_{ij}\left(x_i, x_j\right) = \sum_{k=1}^{N} g_{ik}\left(x_i\right) g_{jk}\left(x_j\right) \tag{21}
$$

where $N$ is the number of expansion term which is related to the approximation accuracy. To this point, the simulation of field $\boldsymbol{\omega}\left(\mathbf{x}\right)$ is converted to the determination of sets of deterministic functions $g_{ij}\left(x_i\right)$ and the corresponding random variables $\eta_j$ in Eq.(19) such that covariance in Eqs.(20) and (21) could match the target one. Since all components of the cross-correlated random fields $\boldsymbol{\omega}\left(\mathbf{x}\right)$ share an identical set of random variables, it becomes feasible to simultaneously represent all correlation structure of the fields, and also, it is natural to firstly determine the sets of functions $g_{ij}\left(x_i\right)$ associated with each component of fields $\boldsymbol{\omega}\left(\mathbf{x}\right)$, and then the set of variables $\eta_j$ in practice.

### 3.2. Finite element discretization of cross-correlated random fields

It is known that, even in the most used KL expansion, the set of deterministic functions are difficult to solve analytically except for a few covariance functions defined on domains $\mathcal{D}$ of simple geometric shape. By relaxing the orthogonality restriction in the presented stochastic expansion, the determination of such functions is more challenging. In order to overcome this obstacle, we approximate $g_{ij}\left(x_i\right)$ in terms of a set of basis functions $N_k\left(x_i\right)$:

$$
g_{ij}\left(x_i\right) = \sum_{k=1}^{N_i} g_{ijk} N_k\left(x_i\right) \tag{22}
$$

where $\left\{g_{ijk}\right\}_{k=1}^{N_i}$ are a set of coefficients to be determined, and $N_k\left(x\right)$ is selected as shape functions in the finite element discretization of domain $\mathcal{D}$, typically piecewise linear polynomial, having the property $N_k\left(\mathbf{x}_l\right) = \delta_{kl}$. The advantage behind this choice is that the resulting approximation in Eq.(22) can be readily embedded into the framework of commonly used shape function discretization scheme. By direct application of Eq.(22), each component of the cross-correlated random fields, $\omega_i\left(x_i\right)$, is further written as

$$
\begin{aligned}
\omega\left(x_i\right) &= \sum_{j=1}^{N_i}\sum_{k=1}^{N_j} g_{ijk} N_k\left(x_i\right)\eta_j \\
&= \sum_{k=1}^{N_i} N_k\left(x_i\right)\left(\sum_{j=1}^{N_i} g_{ijk}\eta_j\right) = \sum_{k=1}^{N_i} N_k\left(x_i\right) W_{ik}
\end{aligned} \tag{23}
$$

where $W_{ik} = \sum_{j=1}^{N} g_{ijk}\eta_j$ is referred to the $k$-th nodal random variable of component $\omega_i\left(x_i\right)$. The truncated version of Eq.(23) accordingly yields

$$\hat{\omega}(x_i) = \sum_{k=1}^{N_i} N_k(x_i)\hat{W}_{ik} \tag{24}$$

where the approximated nodal random variable becomes $\hat{W}_{ik} = \sum_{j=1}^{N} g_{ijk}\eta_j$, and $N$ is the number of truncation terms. Obviously, Eq.(23) discretizes the continuous random field $\omega_i(x_i)$ over each finite element mesh by a combination of the element shape functions and of the nodal random variables representing the random field at the nodes of the mesh, leading to a nodal random vector $\mathbf{W}_i = \{W_{ik}\}_{k=1}^{N_i}$. After approximating all components of $\boldsymbol{\omega}(\mathbf{x})$ in the same manner, a discretized version of the cross-correlated random fields is obtained as

$$\mathbf{W} = \{\mathbf{W}_1, \cdots \mathbf{W}_n\} \tag{25}$$

whose covariance matrix is given by

$$\mathbf{C}_{ij} = \mathbb{E}\left[\mathbf{W}_i \mathbf{W}_j\right] = \left[C_{ij}(x_i, x_j)\right]_{N_i \times N_j} \quad (1 \le i \le j \le n) \tag{26}$$

where covariance matrix $C_{ij}(x_i, x_j)$ with dimension $N_i \times N_j$ is the discretized version of covariance function of the field $\boldsymbol{\omega}(\mathbf{x})$. We emphasize that accuracy of the approximation in both $\mathbf{W}$ and $\mathbf{C}_{ij}$ depends on the discretization of domain $\mathcal{D}$ from finite element mesh, as shown in Eq.(22). Although adaptive discretization procedure based on iterative mesh refinement, as well as the choice of high-order shape functions can lead to a more accurate approximation, the application of such techniques is outside the scope of this paper.

It can directly been seen that, with the aid of the finite element discretization scheme in Eq.(25), the problem is further converted to the determination of sets of coefficients $\{g_{ijk}\}_{k=1}^{N_i}$ such that the discretized covariance matrix in Eq.(26) could match the target covariance. To this end, we assemble all covariance matrices $\mathbf{C}_{ij}\ (1 \le i \le j \le n)$ of order $N_i \times N_j$ into matrix $\mathbf{C}$, which defines the correlation structure among all components of cross-correlated random field $\boldsymbol{\omega}(\mathbf{x})$,

$$\mathbf{C} = \begin{pmatrix} \mathbf{C}_{11} & \mathbf{C}_{12} & \cdots & \mathbf{C}_{1n} \\ \mathbf{C}_{21} & \mathbf{C}_{22} & \cdots & \mathbf{C}_{2n} \\ \vdots & & \ddots & \vdots \\ \mathbf{C}_{n1} & \mathbf{C}_{n2} & \cdots & \mathbf{C}_{nn} \end{pmatrix} \tag{27}$$

where elements $\mathbf{C}_{ij}$ are defined in Eq.(26). Note that dimension of covariance matrix $\mathbf{C}$ is thus $P \times P$, where $P = \sum_{i=1}^{n} N_i$. By definition, covariance matrix is bounded and non-negative definite. Then, matrix $\mathbf{C}$ has the spectral decomposition

$$\mathbf{C} = \mathbf{T}^T \boldsymbol{\Lambda} \mathbf{T} \tag{28}$$

where $\boldsymbol{\Lambda}$ and $\mathbf{T}$ are eigenvalue and eigenvector matrices of $\mathbf{C}$, respectively, obtaining from the solution of matrix eigenvalue problem. As a direct consequence of the spectral decomposition in Eq.(28), we have $\mathbf{G} = \boldsymbol{\Lambda}^{1/2}\mathbf{T}$, where matrix $\mathbf{G}$ is assembled by the sets of $g_{ijk}\ (1 \le i \le n, 1 \le j \le P, 1 \le k \le N_i)$ as

$$\mathbf{G} = \begin{pmatrix} \overbrace{g_{111} \cdots g_{11N_1}}^{N_1} & \cdots & \overbrace{g_{i11} \cdots g_{i1N_i}}^{N_i} & \cdots & \overbrace{g_{n11} \cdots g_{n1N_n}}^{N_n} \\ \vdots & \ddots & \vdots & \ddots & \vdots \\ g_{1P1} \cdots g_{1PN_1} & \cdots & g_{iP1} \cdots g_{1PN_i} & \cdots & g_{nP1} \cdots g_{nPN_n} \end{pmatrix} \tag{29}$$

In this way, the sets of unknown coefficients $g_{ijk}$ associated with each component of cross-correlated random filed $\boldsymbol{\omega}(\mathbf{x})$ can be determined in a quite straightforward manner.

Note that the number of random variables retained in the stochastic expansion dominates the computational demand in the simulation of cross-correlated random fields, and more importantly in subsequent probabilistic investigation, i.e., stochastic finite element analysis. Although a larger value of *N* implies a better representation of field $\boldsymbol{\omega}(\mathbf{x})$, the computational effort in the discretization phase and the subsequent stochastic analysis may increase prohibitively. Therefore, the value of *N* in Eq.(29) should be carefully chosen such that the discretized field $\mathbf{W}$ in Eq.(25) achieves sufficient approximation accuracy with the number of *N* as small as possible. By ordering the eigenvalues in matrix $\boldsymbol{\Lambda}$ according to their magnitude, and accordingly adjusting the order of columns in matrix $\mathbf{T}$, eigenvalue matrix $\boldsymbol{\Lambda}$ and eigenvector matrix $\mathbf{T}$ can be partitioned under the form:

$$\boldsymbol{\Lambda} = \begin{pmatrix} \boldsymbol{\Lambda}_1 & \\ & \boldsymbol{\Lambda}_2 \end{pmatrix}, \quad \mathbf{T} = \begin{pmatrix} \mathbf{T}_1 \\ \mathbf{T}_2 \end{pmatrix} \tag{30}$$

which will be used for dimension reduction in the simulation of cross-correlated random fields. By Eq.(30), spectral decomposition of matrix $\mathbf{C}$ in Eq.(28) is further written as

$$\mathbf{C} = \mathbf{T}_1^T \boldsymbol{\Lambda}_1 \mathbf{T}_1 + \mathbf{T}_2^T \boldsymbol{\Lambda}_2 \mathbf{T}_2 \tag{31}$$

with the property

$$\begin{aligned} & trace(\mathbf{C}) = trace\left(\mathbf{T}_1^T \boldsymbol{\Lambda}_1 \mathbf{T}_1\right) + trace\left(\mathbf{T}_2^T \boldsymbol{\Lambda}_2 \mathbf{T}_2\right) \\ & = trace\left(\boldsymbol{\Lambda}_1\right) + trace\left(\boldsymbol{\Lambda}_2\right) \\ & = \sum_{i=1}^{N} \lambda_i + \sum_{i=N+1}^{P} \lambda_i \end{aligned} \tag{32}$$

where $\lambda_i, i = 1,...,N$ and $\lambda_i, i = N+1,...,P$ are elements of matrices $\boldsymbol{\Lambda}_1$ and $\boldsymbol{\Lambda}_2$, respectively, ordering in a descending manner $\lambda_1 \geq \lambda_2 \geq ... \geq \lambda_P$. Since the largest eigenvalues and their corresponding eigenvectors dominate the decomposition, the second part of the right side of Eq.(31) can be neglected in practical implementation, and the approximate spectral decomposition of the assembled discretized covariance $\mathbf{C}$ reduces to

$$\mathbf{C} \approx \hat{\mathbf{C}} = \mathbf{T}_1^T \boldsymbol{\Lambda}_1 \mathbf{T}_1 = \hat{\mathbf{G}}^T \hat{\mathbf{G}} \tag{33}$$

where $\hat{\mathbf{G}} = \boldsymbol{\Lambda}_1^{1/2} \mathbf{T}_1$ is an $N \times P$ matrix assembled by the sets of $g_{ijk}$ $\left(1 \leq i \leq n, 1 \leq j \leq N, 1 \leq k \leq N_i\right)$ as

$$\hat{\mathbf{G}} = \begin{pmatrix} \overbrace{g_{111} \cdots g_{11N_1}}^{N_1} & \cdots & \overbrace{g_{i11} \cdots g_{i1N_i}}^{N_i} & \cdots & \overbrace{g_{n11} \cdots g_{n1N_n}}^{N_n} \\ \vdots & \ddots & \vdots & \ddots & \vdots \\ g_{1N1} \cdots g_{1NN_1} & \cdots & g_{iN1} \cdots g_{1NN_i} & \cdots & g_{nN1} \cdots g_{nNN_n} \end{pmatrix} \tag{34}$$

Thus, the proper choice of value *N* can be achieved according the target approximation accuracy, for example,

$$\frac{trace\left(\mathbf{T}_1^T \boldsymbol{\Lambda}_1 \mathbf{T}_1\right)}{trace(\mathbf{C})} \geq 0.95 \tag{35}$$

Obviously, by retaining dominant components in the above decomposition, a large amount of computer memory can be saved at a given level of approximation accuracy. With the above-developed dimension reduction technique, the sets of coefficients $g_{ijk}$, as well as the optimal number of these coefficients, can be determined to represent all components of the discretized cross-correlated random field in Eq.(25).

### 3.3. Iteration algorithm for non-Gaussian cross-correlated fields simulation

Once having the deterministic part in Eq.(23) solved, approximation accuracy of the field $\boldsymbol{\omega}(\mathbf{x})$ depends solely on the quality of the set of random variables $\{\eta_j\}$. If the cross-correlated random fields are Gaussian, the set of $\{\eta_j\}$ are independent standard Gaussian random variables. However, if the field $\boldsymbol{\omega}(\mathbf{x})$ is non-Gaussian distributed, distributions of variables $\{\eta_j\}$ are unknown *a prior*, and numerical algorithms have to be developed to approximate these variables. In the context of the above developed methodology, the procedure for determining non-Gaussian KL variables for a random field in [19,20] is further extended to determine non-Gaussian $\{\eta_j\}$ in cross-correlated fields. By virtue of the property that all components of field $\boldsymbol{\omega}(\mathbf{x})$ share a set of same random variables, an effective iterative algorithm for digitally generation of random realizations of $\{\eta_j\}$ in Eq.(23) is developed as follows:

**Step 1:** Generate a total of $M$ samples of $P$-dimensional non-Gaussian random vectors $\mathbf{W}=[\mathbf{W}_1,\mathbf{W}_2,\cdots,\mathbf{W}_n]^T$, whose elements are calculated as

$$\hat{W}_{ik}^{(l)}(\theta_m)=\sum_{j=1}^{N} g_{ijk}\eta_i^{(l)}(\theta_m),\quad m=1,2,\cdots,M \tag{36}$$

where $l$ is the iteration number, and $m$ is the sample number.

**Step 2:** Estimate the simulated covariance matrix and marginal cumulative distribution functions (CDF) as

$$\hat{\mathbf{C}}^{(l)}=\frac{\hat{\mathbf{W}}^{(l)T}(\theta)\hat{\mathbf{W}}^{(l)}(\theta)}{M-1}-\frac{\hat{\mathbf{W}}^{(l)T}(\theta)\mathbf{U}\mathbf{U}^T\hat{\mathbf{W}}^{(l)}(\theta)}{M(M-1)} \tag{37}$$

and

$$\hat{F}_i^{(l)}(y|x)=\frac{1}{M}\sum_{m=1}^{M}\mathbb{I}\left(\mathbf{W}_i^{(l)}(\theta_m)\le y\right),\quad i=1,2,\cdots n \tag{38}$$

where $\mathbf{U}$ is a $M$-dimensional vector whose entries are all one, $y$ indicates the value of empirical distribution function for a non-Gaussian realization, and $\mathbb{I}(\cdot)$ is the indicator function, having the value 1 if event occurs and the value 0 otherwise. We note that the simulated marginal CDF does not necessarily agree with the target one.

**Step 3:** Transform each sample function to match the target marginal cumulative distribution $F_i\,(i=1,2,\cdots,n)$

$$\begin{gathered}\xi^{(l)}(\theta_m)=F_i^{-1}\hat{F}_i^{(l)}\left[\mathbf{W}_i^{(l)}(\theta_m)\right]\\ m=1,\cdots,M;i=1,\cdots,n\end{gathered} \tag{39}$$

and update the next generation of random variables $\eta_j^{(l+1)}(\theta)$ as

$$\eta_j^{(l)}(\theta_m)=\left[\boldsymbol{\xi}^{(l)}(\theta_m)-\overline{\boldsymbol{\xi}}^{(l)}\right]^T\mathbf{g}_j \tag{40}$$

where $\mathbf{g}_j$ is a $P$-dimensional vector with the form

$$\mathbf{g}_j=\left[\overbrace{g_{1j1}\ \cdots\ g_{1jN_1}}^{N_1}\ \cdots\ \overbrace{g_{ij1}\ \cdots\ g_{ijN_i}}^{N_i}\ \cdots\ \overbrace{g_{nj1}\ \cdots\ g_{njN_n}}^{N_n}\right]^T \tag{41}$$

**Step 4:** Steps 1 through 3 are repeated until the sample functions of the field achieve the target marginal CDF.

It is important to noted that, in step 3, the following relation

$$\frac{1}{M-1}\sum_{m=1}^{M}\eta_j(\theta_m)\eta_k(\theta_m)\overset{M\to\infty}{\to}\mathbb{E}\left[\eta_j\eta_k\right]=\delta_{jk} \tag{42}$$

holds for arbitrary two random variables $\eta_j$ and $\eta_k$. This means that uncorrelated random realizations of variables $\eta_j^{(l)}(\theta)$ can be obtained only for an infinite number of sample size $M$, and correlation among variables $\eta_j^{(l)}(\theta)$ would arise with an finite $M$, which is the common case in practice. In order to overcome this difficulty, the rank

orthogonalization scheme developed in [20] is further utilized in this step to reduce the product-moment correlation. According to our experience, a sufficient small correlation coefficient may lead to convergence of the simulated covariance matrix. It will be shown that, with the presented non-Gaussian iteration algorithm, cross-correlated random fields that deviate significantly from the Gaussian case can be handled efficiently just by maintaining target covariance of the fields, and by updating the probability distribution of random variables $\{\eta_j\}$ iteratively.

The resulting procedure for the simulation of cross-correlated random fields is summarized in Algorithm 1, which includes the determination of sets of deterministic functions associated with each component of the field from step 1 to step 6, and the estimation of set of random variables shared by all components of the field from step 7 to step 12. Specifically, the developed algorithm starts from the general stochastic expansion of the cross-correlated random fields in step 1, followed by the finite element discretization of the resulting fields in step 2. By implementing spectral decomposition on the assembled discretized covariance matrix in step 3 and 4, and by further coupling with a dimension technique in step 5, the sets of coefficients $g_{ijk}$ can be straightforwardly obtained in step 6. Note that the optimal number of coefficients $g_{ijk}$ obtained in step 5 has significant importance for the subsequent stochastic analysis because great amount of computational demand can be saved. After having the deterministic coefficients $g_{ijk}$ determined, the corresponding random variables $\{\eta_j\}$ are iteratively estimated from generating samples of non-Gaussian random vector in step 8. By estimating the covariance and marginal CDF from the generated samples in step 9, all samples are then transformed to match the target marginal CDF so that the random variables can be further updated to fit the non-Gaussian CDF in step 10. By repeating step 8 through step 10 until the convergence in step 11 achieved, the set of random variables $\{\eta_j\}$ can thus be iteratively determined to fit the non-Gaussian marginal distribution of all components in the cross-correlated random fields. Once having all the deterministic coefficients $g_{ijk}$ and the corresponding random variables $\{\eta_j\}$ determined, the target cross-correlated random fields can thus be represented in step 13. Since there is no requirement imposed on types of covariances, the presented algorithm is applicable for the simulation of non-stationary fields.

**Algorithm 1** Algorithm for simulating non-Gaussian and non-stationary cross-correlated random fields

1: General stochastic expansion of fields $\boldsymbol{\omega}(\mathbf{x})$ by Eq.(16).
2: Finite element discretization from $\boldsymbol{\omega}(\mathbf{x})$ to $\mathbf{W}$ by Eq.(23).
3: Calculate the discretized covariance matrix $\mathbf{C}_{ij}$ by Eq.(26).
4: Spectral decomposition of covariance matrix $\mathbf{C}$ by Eq.(28).
5: Dimension reduction of $g_{ij}(x)$ by Eq.(31) to Eq.(33).
6: Determine $g_{ijk}$ in Eq.(34).
7: **Repeat**
8: Generate non-Gaussian random vector $\widehat{\mathbf{W}}^{(l)}(\theta)$ by Eq.(36).
9: Calculate covariance $\hat{\mathbf{C}}^{(l)}$ and marginal CDFs $\hat{F}_i^{(l)}$ by Eq.(37) and Eq.(38).
10: Transform random samples to match target marginal CDFs $F_i$ by Eq.(39), and update $\eta_j^{(l+1)}(\theta)$ by Eq.(40).
11: Employ rank orthogonalization scheme to reduce correlations of $\eta_j^{(l+1)}(\theta), (j=1,2,\cdots,N)$.
12: **Until** $\left\|\hat{\mathbf{C}}-\hat{\mathbf{C}}^{(l+1)}\right\| < \epsilon\left\|\hat{\mathbf{C}}\right\|; \hat{F}_i^{(l+1)} = F_i$

13: Simulate cross-correlated random fields $\boldsymbol{\omega}(\mathbf{x})$ by Eq.(24).

As mentioned above, relaxing the orthogonality of deterministic function $g_{ij}(x_i)$ leads to the non-uniqueness of the presented general stochastic expansion in Eq.(19), and thereby enables to simultaneously represent the auto- and cross-correlations of all components of cross-correlated random fields. However, the optimal convergence in mean-square sense can not be achieved due to the nonorthogonality of $g_{ij}(x_i)$, that is, more terms $N$ have to be retained in Eq.(19) to reach a specified accuracy when compared with that in conventional KL expansion. The convergence of general stochastic expansion of all components $\omega_i(x_i), i=1,\cdots,n$ depends on the property of covariance matrix $\mathbf{C}$ in Eq.(27). If the decay of eigenvalues of matrix $\mathbf{C}$ is fast, a reasonable approximation can be achieved with only a small value of $N$, while for matrix $\mathbf{C}$ with slowly decaying eigenvalues, for example, cross-correlated fields with wide-banded evolutionary spectral density function, more terms are required for satisfied accuracy. It is also worth mentioning that the total number of discretized nodes in the finite element discretization of the field, i.e., value of $P$, influence the approximation accuracy of Algorithm 1. Although large values of $P$ may lead to a better representation of cross-correlated random fields, the computational cost of developed method will increase prohibitively, because the spectral decomposition of resulting assembled discretized covariance matrix $\mathbf{C}$ in Eq.(27) can be quite challenging due to the enormous memory and computational resources required. In this case, the state of the art numerical strategies, such as hierarchical matrix technique for large eigenvalue problems in Eq.(33) and higher-order polynomial based Ritz-Galerkin approach for approximating deterministic function $g_{ij}(x_i)$ [26,27], can be introduced to enhance the computational efficiency. In addition, adaptive mesh refinement technique with an error estimator can be further embedded into the developed framework for large-scale engineering problems with different precision requirement [28].

## 4.Extension to the simulation of multi-dimensional random fields

In engineering applications, many environmental loads need to be modeled as multi-dimensional random fields to consider spatially correlated vector time histories of motion occurring simultaneously at different locations. Since there exists an intrinsic relationship between the multi-dimensional fields and cross-correlated fields, as mentioned in [30], we further extend our method to a consistent framework for the simulation of multi-dimensional random fields in this section.

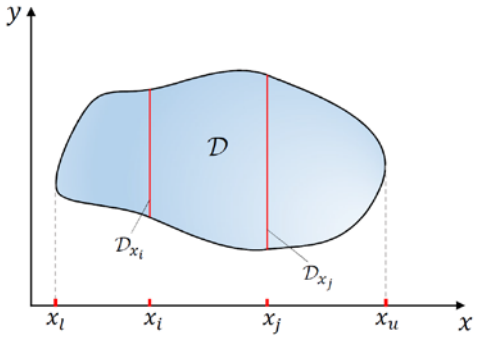

Fig.1. Relationship between domain $\mathcal{D}_{x_i}$ , $\mathcal{D}_{x_j}$ and $\mathcal{D}$

We will conceptually present our method from a two-dimensional random field, and then generalize the method to a multi-dimensional case. Consider a two-dimensional random field $\omega(x,y)$ indexed on a bounded domain $\mathcal{D}$, as shown in Fig.1. Without loss of generality, we assume that the field has a zero mean and a finite covariance function $C(x_1,x_2;y_1,y_2)$, which is bounded for all $x,y\in\mathcal{D}$. It is known that the KL expansion of the field $\omega(x,y)$ is written as

$$\omega(x,y)=\sum_{i=1}^{\infty}\sqrt{\lambda_i}\,f_i(x,y)\xi_i \tag{43}$$

where the eigenvalues $\{\lambda_i\}_{i=1}^{\infty}$ and eigenfunctions $\{f_i(x,y)\}_{i=1}^{\infty}$ are the solution of the following multi-dimensional Fredholm integral equation:

$$\int_{\mathcal{D}} C(x_1,y_1;x_2,y_2)\,f_i(x_2,y_2)\,dx_1dy_1=\lambda_i f_i(x_1,y_1) \tag{44}$$

Since it is generally not feasible to obtain the numerical solution of the Fredholm integral multi-dimensional eigenvalue problem, the KL expansion mostly applied in the simulation of one-dimensional random field in the last few years.

In order to overcome this difficulty, we firstly define a sub-domain $\mathcal{D}_{x_i}\in\mathcal{D}$ by fixing a coordinate $x_i$ on $x$-axis, such that the two-dimensional field $\omega(x,y)$ could be reduced to a one-dimensional random field $\omega(x_i,y)$ for $y\in\mathcal{D}_{x_i}$. Similarly, the two-dimensional field $\omega(x,y)$ can be further converted to a set of one-dimensional fields $\omega(x_j,y)$ for $y\in\mathcal{D}_{x_j}$, by fixing corresponding coordinates $x_j$ on $x$-axis. In this manner, the original two-dimensional random field $\omega(x,y)$ can be discretized to a cross-correlated random fields

$$\omega(x,y)\Leftrightarrow\{\omega(x_l,y),\cdots,\omega(x_i,y),\cdots,\omega(x_u,y)\} \tag{45}$$

whose components are a set of discretized one-dimensional random fields. Obviously, with the increasing of the number of discretized coordinates $x_i$, the resulting cross-correlated random fields better represent the two-dimensional random field $\omega(x,y)$. The second-order correlations between arbitrary two components of the produced cross-correlated fields, i.e., $\omega(x_i,y)$ and $\omega(x_j,y)$, are defined by

$$\begin{cases} C_{x_i}(y_1,y_2)=\mathbb{E}\left[\omega(x_i,y_1)\omega(x_i,y_2)\right] \\ C_{x_j}(y_1,y_2)=\mathbb{E}\left[\omega(x_j,y_1)\omega(x_i,y_2)\right] \\ C_{x_ix_j}(y_1,y_2)=\mathbb{E}\left[\omega(x_i,y_1)\omega(x_j,y_2)\right] \end{cases} \tag{46}$$

Once the two-dimensional field $\omega(x,y)$ is converted to the cross-correlated random field as defined in Eq.(45) and Eq.(46), Algorithm 1 presented in Section 3 can be readily employed for simulating $\omega(x,y)$.

The above method can be straightforwardly extended for the simulation of a multi-dimensional random field, which is summarized in Algorithm 2. Suppose $\omega(x_1,...,x_n)$ is an *n*-dimensional random field indexed on a bounded domain $\mathcal{D}$. By application of the above procedure, the original *n*-dimensional random field $\omega(x_1,...,x_n)$ is firstly converted to a cross-correlated random field whose components are a set of (*n-1*)-dimensional random fields $\omega(x_{1i},...,x_n)$ for $(x_2,...,x_n)\in\mathcal{D}_{x_{1i}}$, where $\mathcal{D}_{x_{1i}}$ is a sub-domain of $\mathcal{D}$. It is seen that dimension of the field is reduced by one in this round of discretization process. Next, each obtained (*n-1*)-dimensional component $\omega(x_{1i},...,x_n)$ is further converted to a new cross-correlated random field whose components are a set of (*n-2*)-dimensional random fields $\omega(x_{1i},x_{2j}...,x_n)$ for $(x_3,...,x_n)\in\mathcal{D}_{x_{2j}}$, where $\mathcal{D}_{x_{2j}}$ is a sub-domain of $\mathcal{D}_{x_{1i}}$. Obviously, the dimension is further reduced by one after this round of discretization process. By further repeating the above dimension reduction process until the cross-correlated random field with a set of one-dimensional components is obtained, Algorithm 1 is then readily

utilized to simulate the resulting cross-correlated random field. It can be deduced that, by multiple application of the method presented in Section 3, the sets of intermediate cross-correlated random fields and thereby the original *n*-dimensional random field $\omega(x_1,...,x_n)$ can be successively simulated in a consistent framework.

**Algorithm 2** A unified framework for simulating multi-dimensional random fields

Define $\mathbf{W}=\varnothing$
**For** $i_1$=1 to $N_{i_1}$ **do**
  **For** $i_2$=1 to $N_{i_2}$ **do**
    …
    **For** $i_n$=1 to $N_{i_n}$ **do**
      $\mathbf{W}=\mathbf{W}\cup\omega(x_{1i_1},\cdots,x_{ni_n})$
    **end for**
    …
  **end for**
**end for**
Simulate **W** by using step 3 to step 12 in Algorithm 1.
Approximate multi-dimensional field $\omega(x_1,\cdots,x_n)$ by **W**.

# 5. Numerical examples

Five illustrative examples demonstrating the application of the proposed method to the synthesis of non-Gaussian and non-stationary cross-correlated random fields, as well as the multi-dimensional random fields, are presented in this section. The first two demonstrate the applicability of the method to stationary cross-correlated random field whose components possess different correlation structures. In the former, the marginal distribution of components of the field are weakly non-Gaussian, while the latter considers a highly non-Gaussian case. These two examples are deliberately chosen to represent the approximate range of non-Gaussian characteristics that are typically met in real-world problems. The third example shows the application to a non-stationary and strongly non-Gaussian cross-correlated random fields. We note that existing KL-based methods, e.g. [21,22], are incapable of simulating these three non-Gaussian cross-correlated fields. In example 4, a two-dimensional random field is used to conceptually illustrate the extension of the developed method in the simulation of a multi-dimensional random field. In the last example, a spatially varying non-Gaussian and nonstationary seismic ground motions is investigated to illustrate the application of proposed method in engineering practice. In all examples, the number of discretized nodes in the finite element discretization of each component of the field is chosen as 100, and the number of expansion terms is chosen as $N=10$, if not mentioned. In addition, the sample size $M$ for the generation of non-Gaussian random variables is adopted as $10^4$. To implement, all computer programs have been run on a notepad (core i5-6300HQ CPU and 16GB RAM).

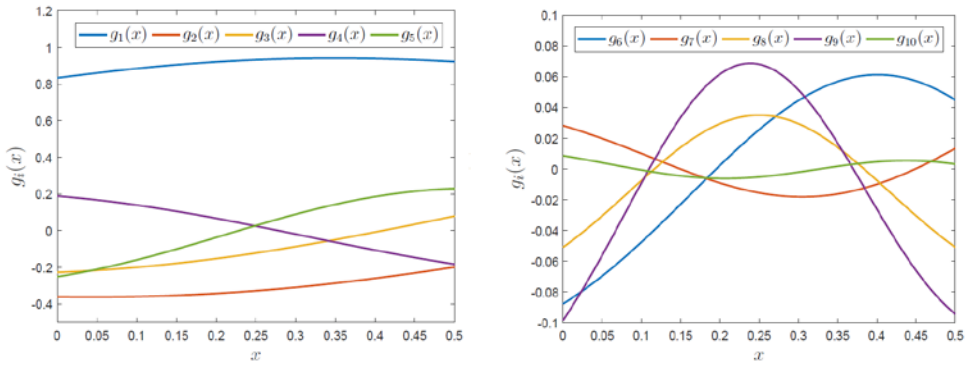


Fig.2. The first ten $g_i(x)$ of $\omega(x)$.

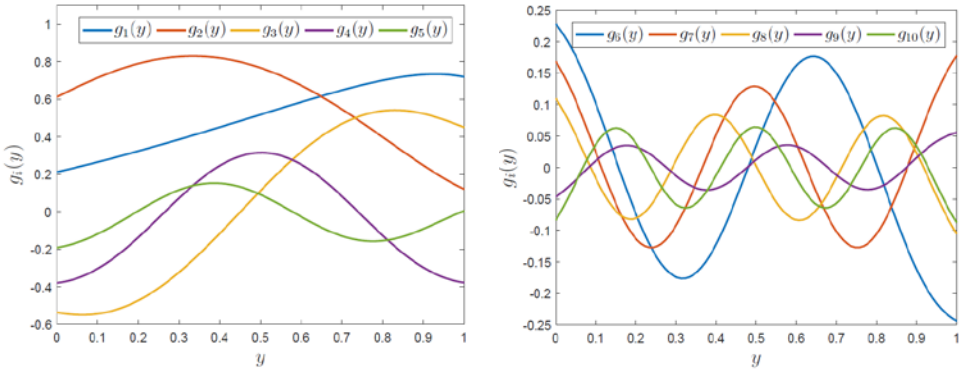


Fig.3. The first ten $g_i(y)$ of $\omega(y)$.

## 5.1. Stationary and weakly non-Gaussian cross-correlated random field with same marginal distribution

In practical engineering implementations, random fields characterized by covariance kernels decaying exponentially is commonly encountered. Unfortunately, this type of covariance kernel has low efficiency with respect to the KL expansion of random fields. In addition, the exponential kernel is not differentiable at its origin, which is not necessarily dictated in experimental data. Therefore, in this section the modified exponential covariance kernel exhibiting enhanced computational efficiency is chosen as auto-correlations of the cross-correlated field [29].

Consider a zero-mean cross-correlated random field $\boldsymbol{\omega} = \{\omega(x), \omega(y)\}$. The covariance function of component $\omega(x)$ is given by

$$C_{xx}(x_1, x_2) = e^{-d|x_1 - x_2|}\left(1 + d|x_1 - x_2|\right), \quad x_i \in \left[0, \frac{1}{2}\right] \tag{47}$$

where $d$ is a parameter that is used to adjust the distance $|x_1 - x_2|$ of null correlation between $\omega(x_1)$ and $\omega(x_2)$. In this example, $d$ is adopted as two. The marginal non-Gaussian CDF of $\omega(x)$ is Beta distributed, with the CDF given by

$$F(x; p, q) = \frac{\Gamma(p+q)}{\Gamma(p)\Gamma(q)} \int_0^u z^{p-1}(1-z)^{q-1}\, dz \tag{48}$$

where $u = (x - x_{\min})/(x_{\max} - x_{\min})$ with upper and lower bounds $x_{\min}$ and $x_{\max}$, and the $\Gamma(\cdot)$ is the Gamma function. The distribution parameters are chosen as $p = 4$ and $q = 2$ so that the mean is zero and the variance is one. Note that the realizations of this distribution are bounded between $x_{\min} = -3.74$ and $x_{\max} = 1.87$. According to [19,20], the target Beta distribution is considered as weakly non-Gaussian and the correlation distortion of this Beta distribution is small. Another component of the field, $\omega(y)$, is a stationary random field with modified exponential covariance given by

$$C_{yy}(x_1, x_2) = e^{-4|x_1 - x_2|}\left(1 + 4|x_1 - x_2|\right), \quad x_i \in [0,1] \tag{49}$$

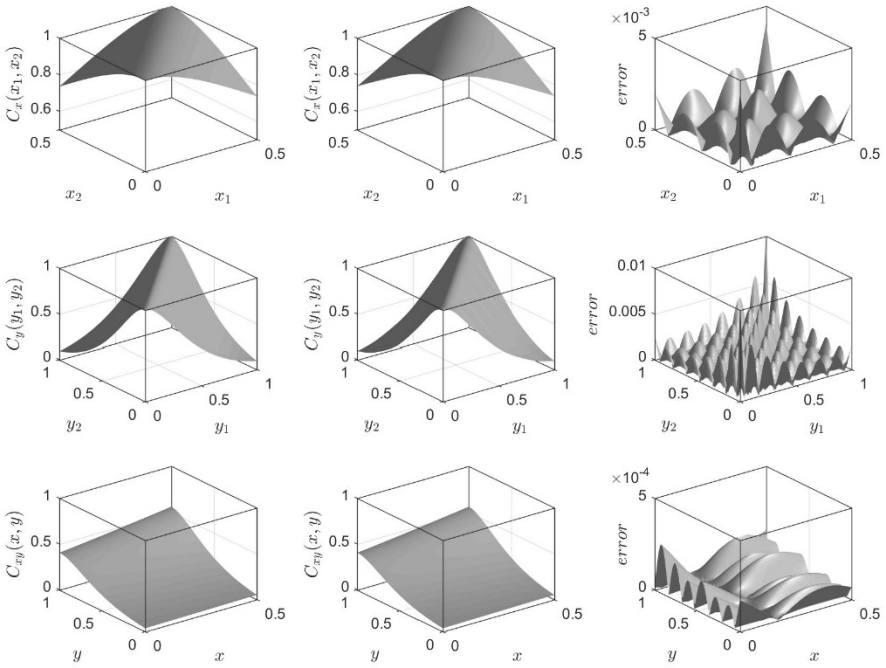

Fig.4. Exact correlations, simulated results and absolute error. (Top: $C_{xx}(x_1,x_2)$; middle: $C_{yy}(y_1,y_2)$; bottom: $C_{xy}(x,y)$.)

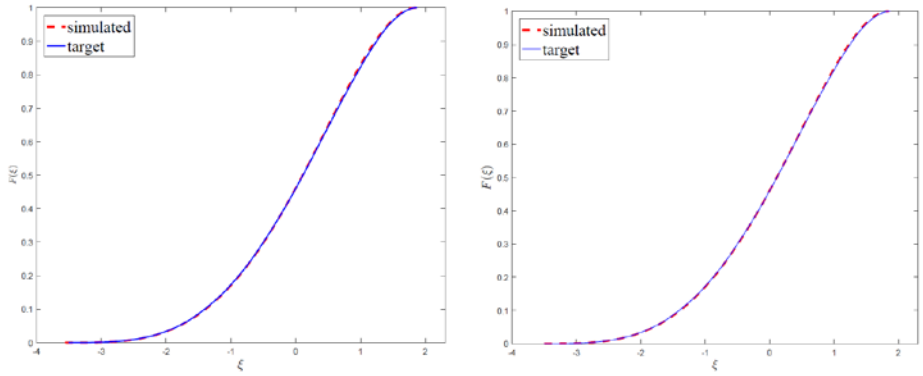


(a). Marginal CDF of $\omega(x)(x=0.25)$ (b). Marginal CDF of $\omega(y)(y=0.5)$

Fig. 5. Exact and simulated marginal CDFs of cross-correlated field $\boldsymbol{\omega}$.

The marginal non-Gaussian CDF of $\omega(y)$ is also Beta distributed, with distribution parameters the same as those in $\omega(x)$. Cross-covariance of the two components, $\omega(x)$ and $\omega(y)$, is given by

$$C_{xy}(x_1,x_2)=e^{-2|x-1|-4|y-1|}\left(1+2|x-1|\right)\left(1+4|y-1|\right) \tag{50}$$

where $x_i\in[0,1/2]$, $y_i\in[0,1]$.

Fig.2 and Fig.3 describe the first ten deterministic functions $\mathrm{g}_i(x)$ and $\mathrm{g}_i(y)$ associated with the stochastic expansion of $\omega(x)$ and $\omega(y)$, respectively. The exact auto-covariance and cross-covariance, the approximated covariances, and the associated errors are shown in Fig.4. It is seen that the approximations of both auto-covariance and cross-covariance agree well with the exact ones although the two components of $\boldsymbol{\omega}$ have the different correlation structure and the different correlation length.

The program converges after two iterations, which only needs 0.48s. Fig.5a and Fig.5b further compare the exact and the approximated marginal CDFs for both components of $\boldsymbol{\omega}$ at $x=0.25$ and $y=0.5$, respectively. It is found that the approximated marginal CDFs are in good accordance with the exact ones for both $\omega(x)$ and $\omega(y)$, illustrating the proposed method could accurately simulate the weakly non-Gaussian cross-correlated fields. No wonder, with the

increase of the values of $N$ and $P$, the approximation accuracy can be further improved.

## 5.2. Stationary and strongly non-Gaussian cross-correlated random field with different marginal distributions

The second example considers a zero-mean cross-correlated random field $\boldsymbol{\omega} = \{\omega(x), \omega(y)\}$. The covariance function of component $\omega(x)$ is given by

$$C_{xx}(x_1, x_2) = \left(1 - |x_1 - x_2|\right), \quad x_i = [0,1] \tag{51}$$

The marginal non-Gaussian CDF of $\omega(x)$ is shifted exponential distributed, with the CDF given by

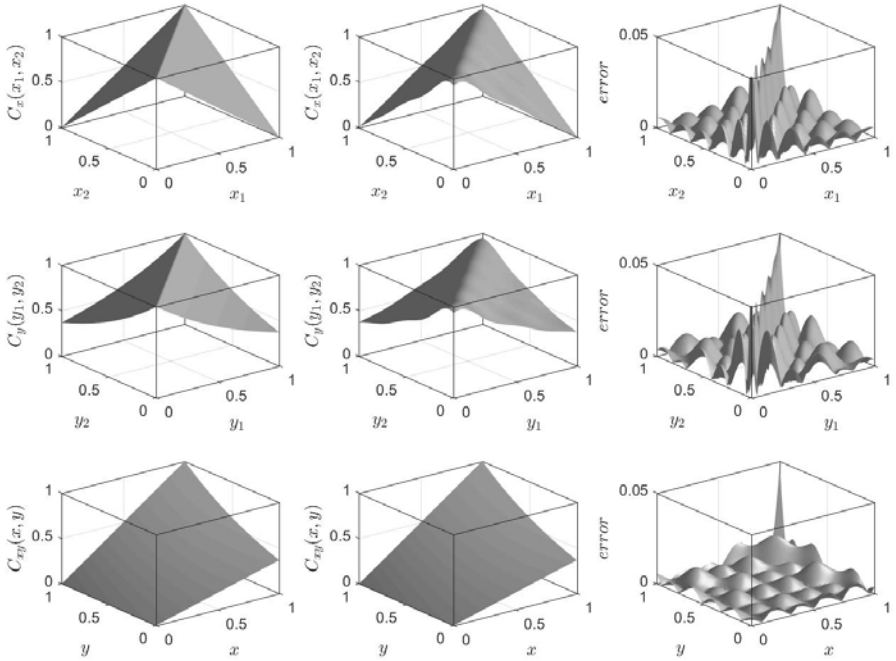


Fig.6. Exact correlations, simulated results and absolute errors. (Top: $C_{xx}(x_1, x_2)$; middle: $C_{yy}(y_1, y_2)$; bottom: $C_{xy}(x, y)$.)

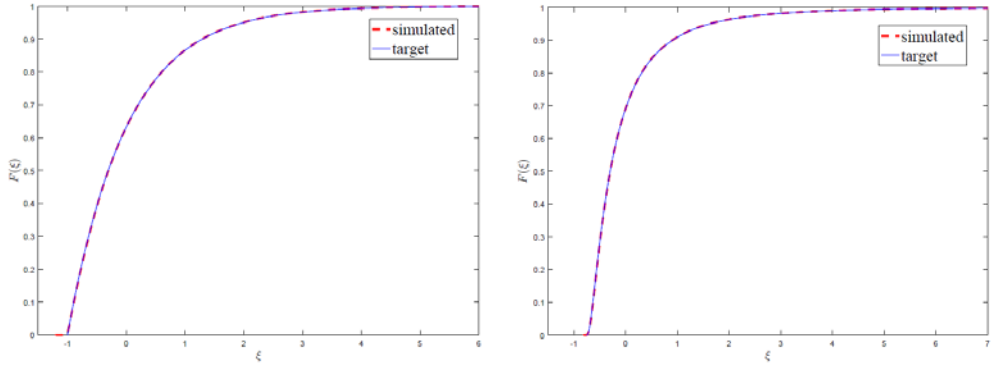


(a). Marginal CDF of $\omega(x)(x = 0.5)$ (b). Marginal CDF of $\omega(y)(y = 0.5)$

Fig. 7. Exact and simulated marginal CDFs of cross-correlated field $\boldsymbol{\omega}$.

$$F(x; \mu, \lambda) = 1 - e^{-\lambda(x-\mu)} \tag{52}$$

The mean and variance of the marginal CDF are

$$\begin{cases} \mu_{SE} = \dfrac{1}{\lambda} + \mu \\ \sigma_{SE}^2 = \dfrac{1}{\lambda^2} \end{cases} \tag{53}$$

In this example, the distribution parameters $\lambda = 1$ and $\mu = -1$ are selected to produce zero mean and unit variance. Another component, $\omega(y)$, is described by the following exponential covariance kernel

$$C_{yy}\left(y_1,y_2\right)=e^{-|y_1-y_2|},\quad y_i=[0,1] \tag{54}$$

The marginal non-Gaussian CDF of $\omega(y)$ is selected as shifted lognormal distribution, whose CDF is given by

$$F\left(x;\mu,\sigma,\delta\right)=\Phi\left(\frac{\ln\left(y-\delta\right)-\mu}{\sigma}\right) \tag{55}$$

with mean and variance

$$\begin{cases}\mu_{SL}=\delta+\exp\left(\mu+\dfrac{\sigma^2}{2}\right)\\ \sigma_{SE}^2=\exp\left(2\mu+\sigma^2\right)\left[\exp\left(\sigma^2\right)-1\right]\end{cases} \tag{56}$$

Distribution parameters $\mu=0.7707$, $\sigma=1$ and $\delta=0.7628$ are selected such that the non-Gaussian CDF has zero mean and unit variance. According to [19,20], the distribution function of both shifted exponential distribution and shifted lognormal distribution deviate significantly from the Gaussian case, and thus can be considered as strongly non-Gaussian. Cross-correlation between $\omega(x)$ and $\omega(y)$ is defined by

$$C_{xy}\left(x,y\right)=e^{-|y-1|}\left(1-|x-1|\right),\quad (x,y)\in[0,1]\times[0,1] \tag{57}$$

The program converges after four iterations, which only needs 1.02s. The exact covariances, the approximated covariances, and the associated errors are compared in Fig.6. Similar observations can be found as Example 1, the approximations of both auto-covariance and cross-covariance generally agree well with the exact ones, illustrating the effectiveness of the proposed method in the representation of correlation structures for cross-correlated random field $\boldsymbol{\omega}$. Fig.7 depicts the exact and the approximated marginal CDFs for both components of $\boldsymbol{\omega}$ at $x=0.5$ and $y=0.5$, respectively. Similar as the results in Example 1, the approximated marginal CDFs once again achieve very good match with the exact ones even for strongly non-Gaussian marginal distributions. Results of the above-two examples indicate the success of the proposed method in the simulation of strongly non-Gaussian cross-correlated fields with different marginal distributions.

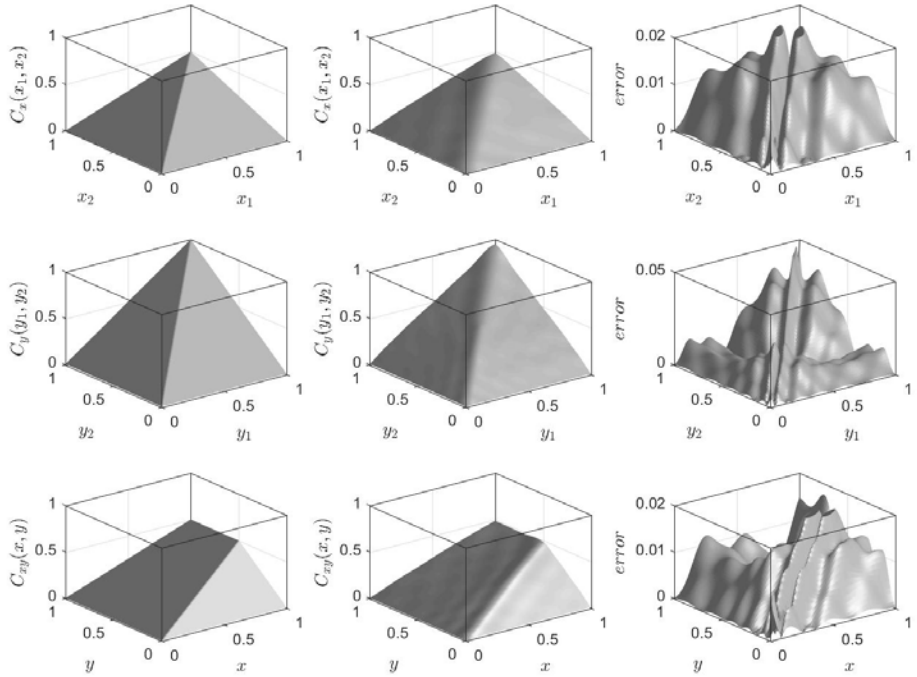


Fig.8. Exact correlations, simulated results and absolute errors.(Top: $C_{xx}\left(x_1,x_2\right)$; middle: $C_{yy}\left(y_1,y_2\right)$; bottom: $C_{xy}\left(x,y\right)$.)

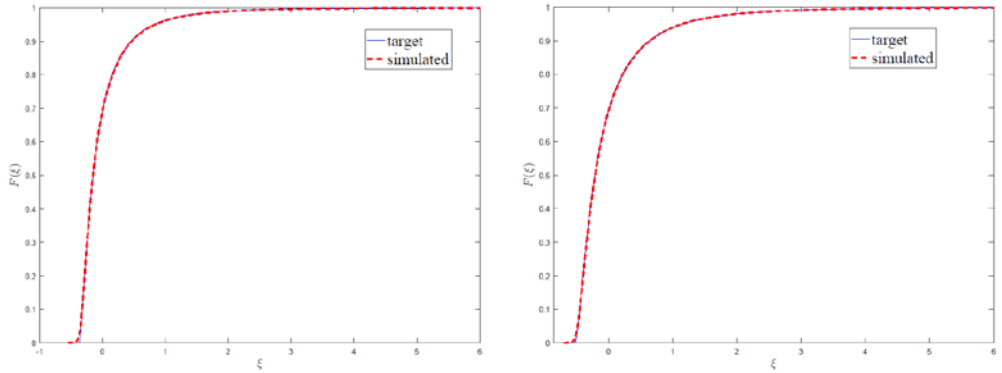


(a). Marginal CDF of $\omega(x)(x=0.5)$ (b). Marginal CDF of $\omega(y)(y=0.5)$

Fig. 9. Exact and simulated marginal CDFs of cross-correlated field $\boldsymbol{\omega}$.

## 5.3. Non-stationary and strongly non-Gaussian cross-correlated field

In order to further examine the capacity of the proposed method in dealing with non-stationary cross-correlated random fields, which is the common case in practice, the third example considers a zero-mean cross-correlated random field $\boldsymbol{\omega}=\{\omega(x),\omega(y)\}$. Covariance functions of both components of the field are given by

$$C_{xx}(x_1,x_2)=0.5\min(x_1,x_2),\quad x_i=[0,1] \tag{58}$$

and

$$C_{yy}(y_1,y_2)=\min(y_1,y_2),\quad y_i=[0,1] \tag{59}$$

Cross-correlation between two components of the field, $\omega(x)$ and $\omega(y)$, is defined by

$$C_{xy}=\min(0.5x,y),\quad (x,y)\in[0,1]\times[0,1] \tag{60}$$

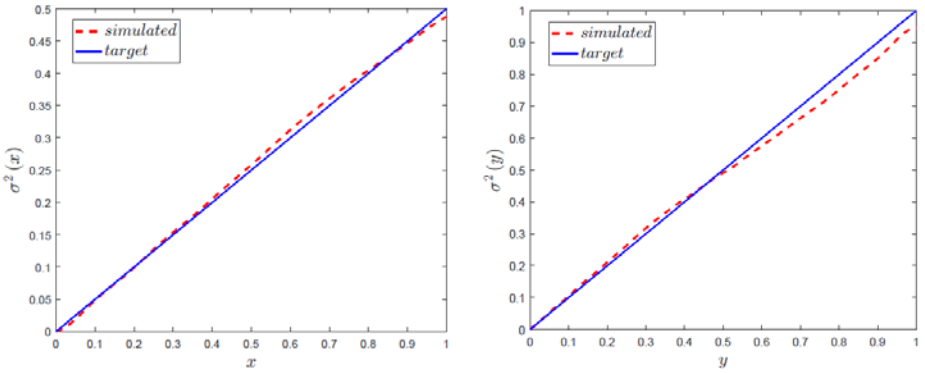


Fig.10. Exact variance v.s. simulated variance of cross-correlated field $\boldsymbol{\omega}$. Left: $\omega(x)$. Right: $\omega(y)$.

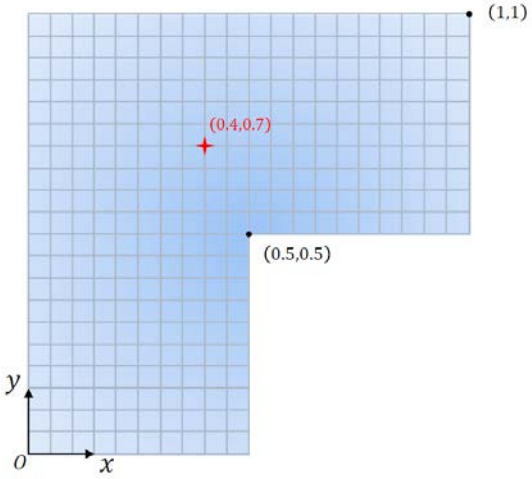


Fig.11. Description of example 4: L-shaped spatial domain $\Omega$

Since both auto-covariances and cross-covariance are of the type of Wiener-Levy fields, this example can be used to investigate the performance for simulating a non-stationary cross-correlated field. The marginal non-Gaussian CDF of $\omega(x)$ is shifted log-normal distributed, with the CDF given by

$$F(x;\mu,\sigma,\delta)=\Phi\left(\frac{\ln\left(y-\delta(x)\right)-\mu(x)}{\sigma}\right) \tag{61}$$

where the shape parameter $\sigma$ is chosen to be one, the scaling parameter and the position parameter are respectively chosen as $\mu(x)=\frac{1}{2}\ln(0.5x)-0.7707$ and $\delta(x)=\sqrt{0.291x}$, so that the target mean of the distribution is zero, i.e.,

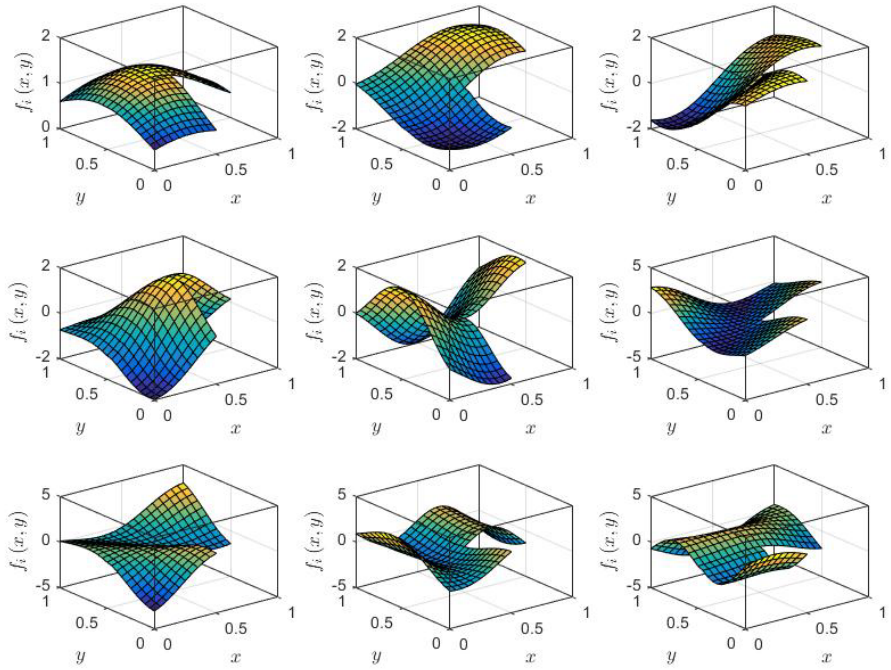


Fig.12. The first nine approximated eigenfunctions of $\kappa(x,y)$.

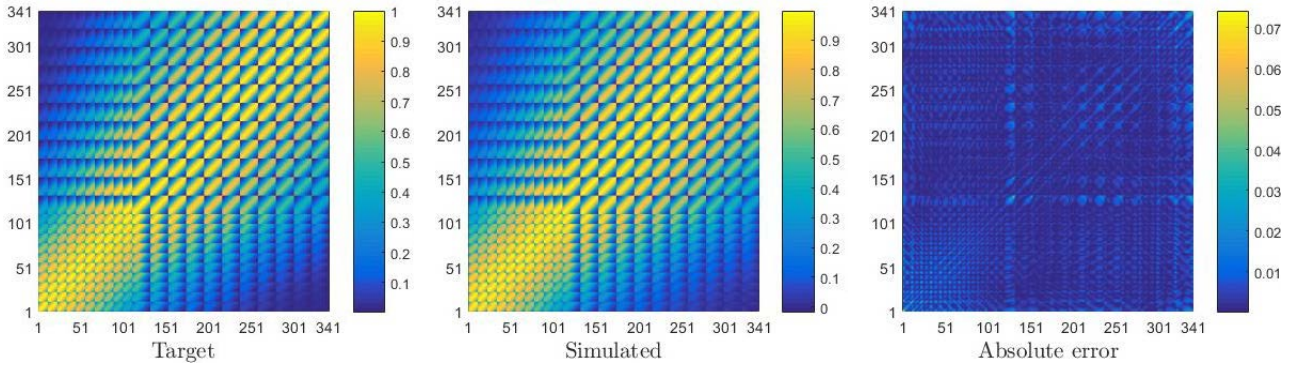


Fig.13. Exact correlations, simulated results and absolute errors.

$$\mu_{SL}=\delta+\exp\left(\mu+\frac{\sigma^2}{2}\right)=0 \tag{62}$$

In such a case, the target variance of the distribution becomes

$$\sigma_{SE}^2=\exp\left(2\mu+\sigma^2\right)\left[\exp\left(\sigma^2\right)-1\right]=\frac{1}{2}C_{xx}(x,x)=\frac{1}{2}x \tag{63}$$

The marginal CDF of $\omega(y)$ is also shifted log-normal distributed, with the distribution parameters given by

$$\begin{cases} \sigma = 1 \\ \mu(y) = \dfrac{1}{2}\ln(y) - 0.7707 \\ \delta(y) = \sqrt{0.582y} \end{cases} \tag{64}$$

Thus the target mean of the distribution is zero, and the target variance can be obtained as

$$\sigma_{SE}^2 = \exp\left(2\mu + \sigma^2\right)\left[\exp\left(\sigma^2\right) - 1\right] = C_{yy}(y, y) = y \tag{65}$$

The program converges after five iterations, which only needs 1.57s. The exact covariances, the approximated covariances, and the associated errors are compared in Fig.8. Although the approximation accuracy is not as good as that in the stationary cases (i.e., results in Example 1 and 2), quality of the approximation is sufficient for simulating non-stationary covariance kernels in practice. If higher accuracy is desired, one can increase the number of $N$ and $P$ in the stochastic expansion. Fig.9 shows the exact and the approximated marginal CDFs for both components of $\boldsymbol{\omega}$ at $x = 0.5$ and $y = 0.5$, respectively. Again, the approximated marginal CDFs are in good accordance with the exact ones for strongly non-Gaussian marginal distributions. Since variance of the marginal CDF depends on its argument in a non-stationary case, we further compare the exact variance and the approximate one of marginal CDF of the two components in Fig.10, respectively. It can be found that there is a small deviation between the approximated variance and the exact one for both cases. Nevertheless, the approximation accuracy is satisfactory for the whole distribution, demonstrating the high accuracy of the proposed method in the simulation of non-stationary and strongly non-Gaussian cross-correlated random fields.

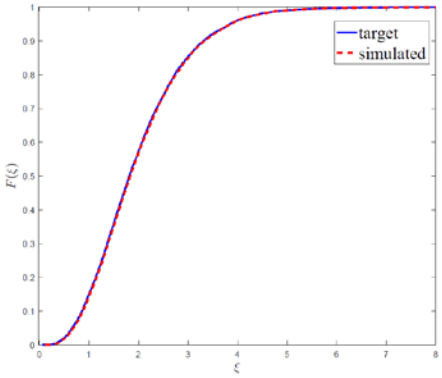


Fig.14. Target CDF v.s. simulated CDF $(x = 0.4, y = 0.7)$.

## 5.4. A two-dimensional random field with exponential covariance

In this example, a two-dimensional random field is considered to illustrate the extension of the proposed method in the simulation of a multi-dimensional random fields by conceptually establishing the relation between cross-correlated field and multi-dimensional field. We note that this field can also be directly discretized by combining two-dimensional shape functions with corresponding nodal random vector. Consider a classical stationary heat diffusion problem defined on a L-shaped spatial domain $\Omega$ (see Fig.11). Volumic heat source is imposed on $\Omega$. The conductivity parameter $\kappa$ is modeled as a two-dimensional random field $\kappa(x, y)$ with the exponential covariance given by

$$C(x_1, x_2, y_1, y_2) = \exp\left(-\frac{(x_1 - x_2)^2 + (y_1 - y_2)^2}{L^2}\right) \tag{66}$$

where $L = 0.5$ for $(x_i, y_i) \in \Omega$. The marginal CDF of $\kappa(x, y)$ is Gamma distributed, with the CDF given by

$$F(x;\alpha,\beta)=\int_0^x \frac{z^{\alpha-1}e^{-z/\beta}}{\beta^{\alpha}\Gamma(\alpha)}dz \tag{67}$$

where distribution parameters are selected as $\alpha=4$, and $\beta=0.5$, and symbol $\Gamma$ denotes the Gamma function.

As described in Algorithm 2, the proposed method needs to convert a *n*-dimensional random field to a cross-correlated random field whose components are a set of (*n-1*)-dimensional random fields. In this example, the 2-dimensional conductivity field $\kappa(x,y)$ is discretized at a set of equally spaced coordinates $y_i$ on *y*-axis, i.e., $\Delta y \equiv y_{i+1}-y_i=0.05$, leading to a cross-correlated field

$$\kappa(x,y)\Leftrightarrow\left\{\kappa(x,y_i)\right\}_{i=1}^{21} \tag{68}$$

with components being one-dimensional fields. The correlation of the resulting cross-correlated random field is then defined by a total of $21(21+1)/2=231$ covariance functions which is specified by Eq.(66). Once having the multi-dimensional field converted to the cross-correlated field, the proposed method can be readily used for the simulation of cross-correlated field derived in Eq.(68), and thereby the conductivity field $\kappa(x,y)$. In this context, finite element approximation is used to discretize each component $\kappa(x,y_i)$ with step size $\Delta x=\Delta y=0.05$, so that the resulting dimension of the problem becomes 341. The program converges after three iterations, which only needs 0.93s. The approximated first nine eigenfunctions of the 2-dimensional conductivity field $\kappa(x,y)$ are depicted in Fig.12. The exact covariances, the approximated covariances, and the associated errors are compared in Fig.13. Similar observations can be found as the previous examples, the approximations of covariance functions are in very good accordance with the exact ones, validating the proposed method in the simulation of multi-dimensional fields. Fig.14 shows the exact and the approximated marginal CDFs at point $(0.4,0.7)$ (red star in Fig.11). The high approximation accuracy once again demonstrates the developed non-Gaussian iteration algorithm even in a multi-dimensional case.

### 5.5. A spatially varying non-Gaussian and nonstationary seismic ground motions

Consider the seismic ground motions which occur at three locations on the ground surface along the line spatially located at 0, 100 and 200m. The acceleration time histories are modelled as a tri-variate nonstationary process $\mathbf{X}(t)=(X_1(t),X_2(t),X_3(t))$ with the same evolutionary spectrum, i.e., the Kanai-Tajimi acceleration spectrum with Clough-Penzien correction possessing both frequency and amplitude modulation

$$S(\omega,t)=M^2(t)S_0(t)\frac{1+4\zeta_g^2(\omega/\omega_g)^2}{\left[1-(\omega/\omega_g)^2\right]^2+4\zeta_g^2(\omega/\omega_g)^2}\frac{(\omega/\omega_f)^4}{\left[1-(\omega/\omega_f)^2\right]^2+4\zeta_f^2(\omega/\omega_f)^2} \tag{69}$$

where

$$M(t)=\begin{cases}(t/t_1)^2 & 0\le t\le t_1\\ 1 & t_1\le t\le t_2\\ \exp\left[-\lambda(t-t_2)\right] & t\ge t_2\end{cases} \tag{70}$$

$$S_0=\frac{\sigma^2}{\pi\omega_g\left[1/(2\zeta_g)+2\zeta_g\right]} \tag{71}$$

where $\sigma$ is the standard deviation, and $\omega_g$ and $\zeta_g$ are characteristic frequency and damping of the ground, respectively. $\omega_f$ and $\zeta_f$ are the filtering parameters of the Clough-Penzien correction, which are typically taken to be $\omega_f=0.1\omega_g$, $\zeta_f=\zeta_g$. The parameters definitions used in the example are $\sigma=110\,cm/s^{3/2}$, $\omega_g=30-1.25t\,(rad/s)$, $\zeta_g=0.5+0.005t$, $t_1=2s$, $t_2=10s$, and $\lambda=0.4$. The characterized

by following coherency model

$$\left|\gamma_{jk}(\omega)\right| = A\exp\left[-2d_{jk}(1-A+\alpha A)/\alpha\theta(\omega)\right] + (1-A)\exp\left[-2d_{jk}(1-A+\alpha A)/\theta(\omega)\right] \tag{72}$$

where $\theta(\omega) = K\left[1+(\omega/2\pi f_0)^b\right]^{-1/2}$, and $A=0.636$, $\alpha=0.0186$, $K=31200$, $f_0=1.51$ and $b=2.95$. The wave velocity of seismic ground motion is set to be $500\,m/s$. The corresponding auto/cross-correlation functions can be determined by

$$C(t_1,t_2) = \int_{-\infty}^{+\infty}\sqrt{S(\omega,t_1)S(\omega,t_2)}e^{i\omega(t_1-t_2)}d\omega \tag{73}$$

For illustration, Fig.15 shows the auto evolution spectrum along with the corresponding correlation, and Fig.16 shows the module of cross evolution spectrum $S_{12}(\omega,t)$ and the corresponding cross-correlation $C_{12}(t_1,t_2)$.

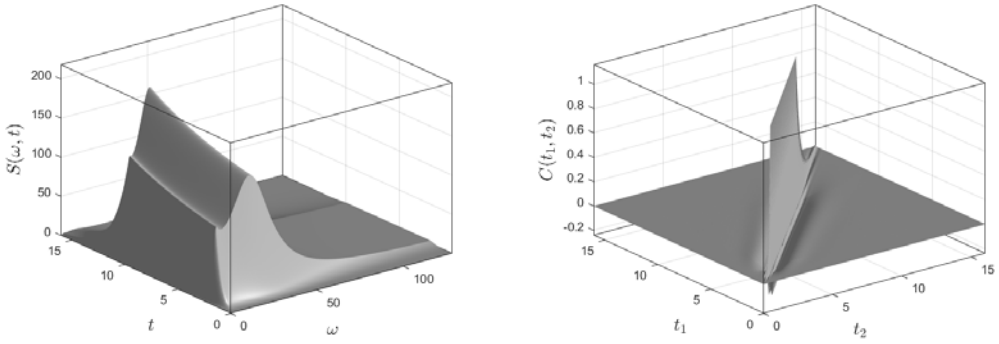


Fig.15 Clough–Penzien spectrum with amplitude and frequency modulation and corresponding non-stationary auto-correlation function: left: evolution spectral; right: auto-correlation function.

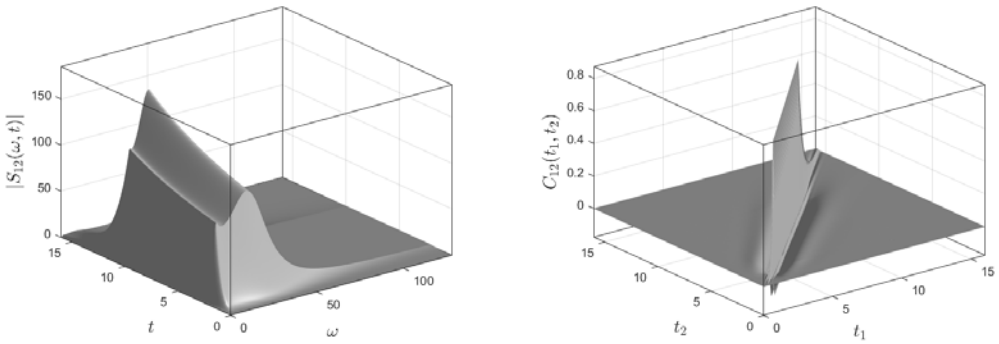


Fig.16: The module of cross evolution spectrum $S_{12}(\omega,t)$ and the corresponding cross-correlation $C_{12}(t_1,t_2)$.left: $\left|S_{12}(\omega,t)\right|$; right: $C_{12}(t_1,t_2)$.

The non-Gaussian marginal distribution of seismic ground motions is the Students's *t*-distribution

$$f(x) = \frac{\Gamma\left((c+1)/2\right)}{b\sqrt{\pi c}\,\Gamma(c/2)}\left[1+\frac{\left((x-a)/b\right)^2}{c}\right]^{-\frac{c+1}{2}} \tag{74}$$

where $a=0$ such that the distribution has zero-mean and skewness. The constant $c$ is adopted as $c=6$ such that the constant $b$ can be determined by $b^2=(c-2)\sigma^2/c$. In this example, a total of 16s seismic ground motions are simulated, and the time is discretized as $\Delta t = 0.04s$. The number of expansion terms in Eq.(19) is chosen as $N=806$ such that 99% energy are retained.

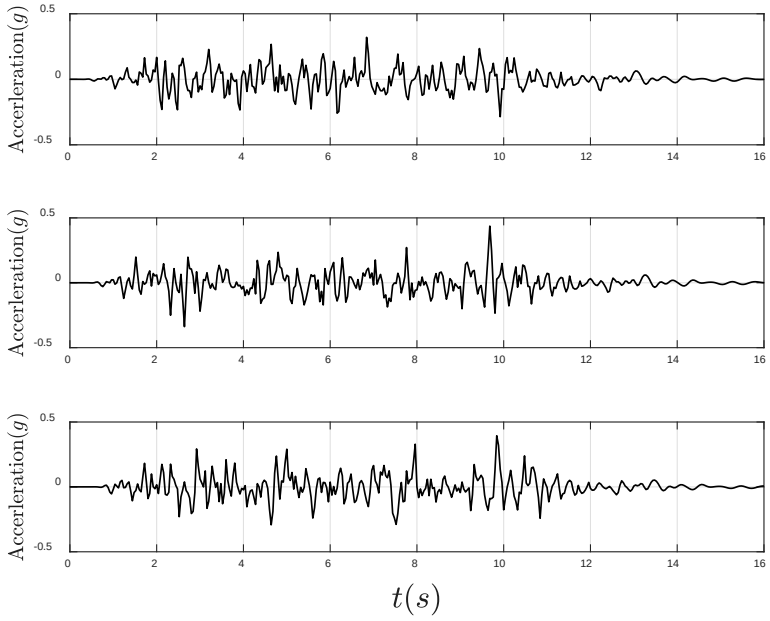


Fig.17 Simulated non-Gaussian seismic ground motions. (Top: $X_1(t)$; middle: $X_2(t)$; bottom: $X_3(t)$.

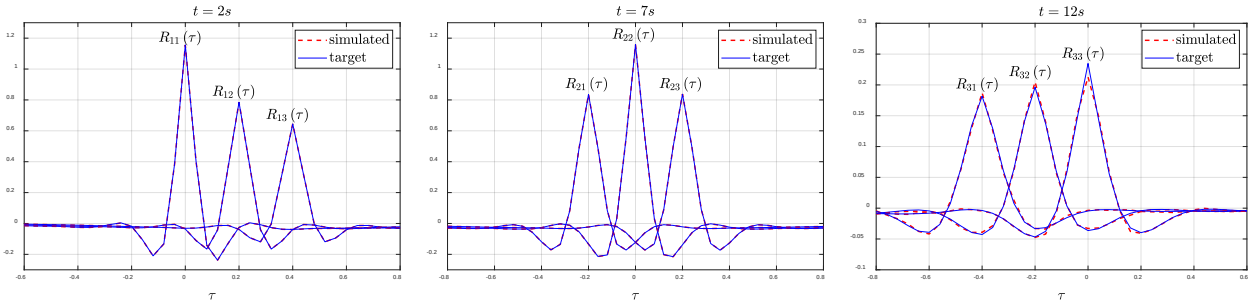


Fig.18 Target auto/cross-correlations and the approximated correlations at some typical time points.

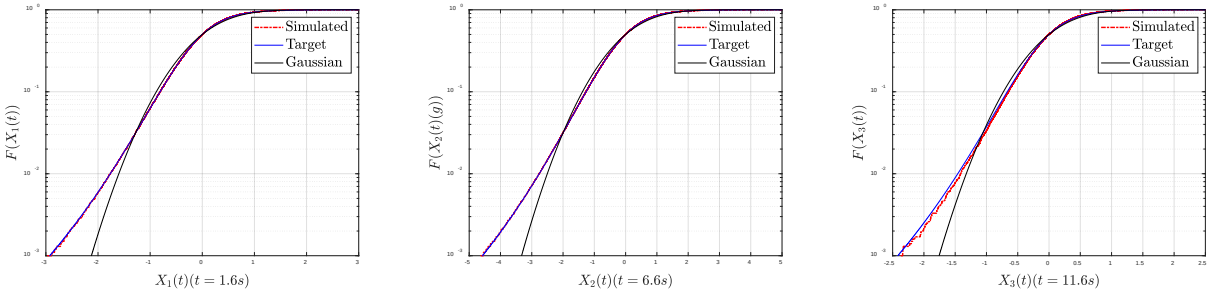


Fig.19 Target CDFs and simulated CDFs of tri-variate seismic process $\mathbf{X}(t)=\left(X_1(t),X_2(t),X_3(t)\right)$ at some typical time points.

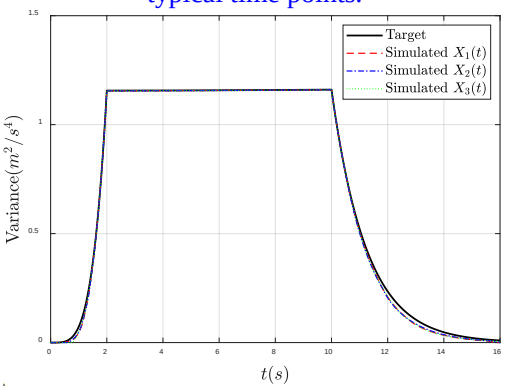


Fig.20 Target and simulated variances of tri-variate seismic process $\mathbf{X}(t)=\left(X_1(t),X_2(t),X_3(t)\right)$.

The program converges after two iterations, which only needs 4.38s. Fig.17 depicts one sample of the simulated non-stationary non-Gaussian seismic ground motions $\mathbf{X}(t)=\left(X_1(t),X_2(t),X_3(t)\right)$. Fig.18 shows the target and the approximated auto/cross-correlations at some typical time points. It is evident that the approximations of both auto-covariance and cross-covariance generally agree well with the exact ones, illustrating the effectiveness of the proposed method in the representation of correlation structures for spatially varying seismic ground motions. Fig.19 depicts the target and the simulated non-Gaussian marginal CDFs of process $\mathbf{X}(t)=\left(X_1(t),X_2(t),X_3(t)\right)$ at some typical time points, the simulated marginal CDFs once again achieve very good match with the exact ones. Since variance of the marginal CDF is time dependent in non-stationary seismic ground motion, we further compare the target and the simulated variances of the three components in Fig.20. It can be found that there is a small deviation between the approximated variances and the exact one. Nevertheless, the approximation accuracy is satisfactory for the whole distribution and can be further improved by retaining more terms $N$ in Eq.(19), demonstrating the high accuracy of the proposed method in the simulation of spatially varying non-Gaussian and nonstationary seismic ground motions.

# 6. Conclusion

A practical framework has been developed for the simulation of non-Gaussian and non-stationary cross-correlated random fields. The developed methodology firstly represents the cross-correlated random fields by means of a general stochastic expansion scheme, in which all components of the fields are expanded under an identical set of random variables. A finite element discretization scheme is subsequently developed to further approximate the fields so that spectral decomposition might be readily utilized on the resulting discretized covariance matrix of the field. By further coupling with a dimension reduction technique, the sets of deterministic functions associated with each component of the fields, together with the optimal number of these functions, can be quite straightforwardly determined. For non-Gaussian identical fields, by virtue of the remarkable property of the general expansion, i.e., all components of the field can be represented under a set of same random variables, an iterative mapping procedure is then developed to fit the non-Gaussian marginal distribution of all components of the field. In this manner, the target field can be efficiently simulated from the presented stochastic expansion scheme, and the developed methodology thereby offers a unified framework for simulating non-Gaussian cross-correlated random fields with arbitrary covariance functions, which need not be stationary. In addition, we further generalize our method to a consistent framework for the simulation of multi-dimensional random fields. Five illustrative numerical examples, including a spatially varying non-Gaussian and nonstationary seismic ground motions, are utilized to demonstrate the effectiveness and range of applicability of the method. In addition to being suitable for simulating cross-correlated random fields, the new method is highly desirable for implementation with the non-intrusive stochastic finite element analysis as well as reliability analysis to a wide class of problems involving multi-correlations.

# Acknowledgments

This research was supported by Grant from the National Natural Science Foundation of China (Project 11972009). These supports are gratefully acknowledged. The authors would like to acknowledge the thoughtful suggestions of three anonymous reviewers, which substantially improved the present paper.

# Appendix

In this appendix, we prove the convergence of the presented general stochastic expansion presented in Section 3.1. In general, global error measures are applied to compare the random field discretization methods and to quantify the overall quality of a random field approximation. In case of the truncated general expansion, the mean square error can be derived by application of the orthogonality of random variables $\eta_i$ as

$$\begin{aligned}\varepsilon_M^2 &= \mathbb{E}\left[\left(\omega(x)-\hat{\omega}(x)\right)^2\right] = \mathbb{E}\left[\omega^2(x)\right] - 2\mathbb{E}\left[\omega(x)\hat{\omega}(x)\right] + \mathbb{E}\left[\hat{\omega}^2(x)\right] \\ &= \sum_{i=1}^{\infty}\sum_{j=1}^{\infty} g_i(x) g_j(x) \mathbb{E}\left[\eta_i\eta_j\right] - 2\sum_{i=1}^{\infty}\sum_{j=1}^{M} g_i(x) g_j(x) \mathbb{E}\left[\eta_i\eta_j\right] + \sum_{i=1}^{M}\sum_{j=1}^{M} g_i(x) g_j(x) \mathbb{E}\left[\eta_i\eta_j\right] \\ &= \sum_{i=1}^{\infty} g_i^2(x) - 2\sum_{i=1}^{M} g_i^2(x) + \sum_{i=1}^{M} g_i^2(x) = \sum_{i=M+1}^{\infty} g_i^2(x)\end{aligned} \tag{75}$$

On the basis of the mean square error as derived in Eq.(75), the convergence of the general stochastic expansion in Eq.(11) is further investigated. To this end, we assume that $\{g_1(x),\cdots,g_M(x)\}$ are a set of linearly independent deterministic functions defined on a bounded interval $\mathcal{D}$, which span a *M*-dimensional subspace $S = span\{g_1(x),\cdots,g_M(x)\}$ of $L^2(\mathcal{D})$. The following propositions summarize essential features of the presented expansion.

**Proposition 1.** *Given a finite set of orthonormal basis* $\{f_1(x),\cdots,f_M(x)\}$ *on the subspace* $S$, *then* $\{g_1(x),\cdots,g_M(x)\}$ *and* $\{f_1(x),\cdots,f_M(x)\}$ *are related by*

$$g_i(x) = \sum_{j=1}^{M} \sqrt{\lambda_j}\, q_{ij}\, f_j(x) \tag{76}$$

*where* $q_{ij}$ *are elements of an orthogonal matrix* $\mathbf{Q}$, *and* $\lambda_j$ *are elements of a diagonal matrix* $\mathbf{\Lambda}$.

**Proof.** By application of property of orthonormal functions, we immediately have

$$g_i(x) = \sum_{j=1}^{M} \alpha_{ij} f_j(x) \tag{77}$$

where $\alpha_{ij} = \alpha_{ji} = \langle g_i(x), f_j(x)\rangle$, equipped with the inner product $\langle\cdot,\cdot\rangle$, such that for $u(x)$ and $v(x)$ in $L^2(\mathcal{D})$,

$$\langle u(x), v(x)\rangle = \int_{\mathcal{D}} u(x) v(x)\, dx \tag{78}$$

Multiplying both sides of Eq.(77) by $g_k(x)$, and integrating over the domain $\mathcal{D}$ with respect to *x*, yields

$$\int_{\mathcal{D}} g_i(x) g_k(x)\, dx = \sum_{j=1}^{M}\sum_{l=1}^{M} \alpha_{ij}\alpha_{kl} \int_{\mathcal{D}} f_j(x) f_l(x)\, dx = \sum_{j=1}^{M} \alpha_{ij}\alpha_{kj} \tag{79}$$

which can be rewritten in a concise form as:

$$\mathbf{G} = \mathbf{A}\mathbf{A}^T \tag{80}$$

where $\mathbf{G} = [G_{ik}]_{M\times M}$ is defined by $G_{ik} = \int_{\mathcal{D}} g_i(x) g_k(x)\, dx$, and $\mathbf{A}$ is an $M \times M$ matrix with elements $\alpha_{ij}$. Obviously, $\mathbf{G}$ is a symmetric and positive definite matrix with real-valued elements. Then, there must exist an orthogonal matrix $\mathbf{Q} = [q_{ij}]_{M\times M}$ and a diagonal matrix $\mathbf{\Lambda} = diag(\lambda_1,\cdots,\lambda_M)$, such that relation $\mathbf{G} = \mathbf{Q}\mathbf{\Lambda}\mathbf{Q}^T$ holds. That is

$$g_i(x) = \sum_{j=1}^{M} \sqrt{\lambda_j}\, q_{ij}\, f_j(x) \tag{81}$$

This completes the proof. □

**Proposition 2.** *Sequence of random field representation* $\{\hat{\omega}_M(x), M = 1,2,\cdots\}$ *converges in mean square (m.s.) to* $\omega(x)$, *i.e.,* $\mathbb{E}\left[\left(\omega(x)-\hat{\omega}_M(x)\right)^2\right] \to 0$, *as* $M \to \infty$, *where* $\hat{\omega}_M(x)$ *denotes the M-th truncated series.*

**Proof.** By substituting the relation between $\{g_1(x),\cdots,g_M(x)\}$ and $\{f_1(x),\cdots,f_M(x)\}$ given in Proposition 1 into

Eq.(14), we have

$$\begin{aligned}\hat{\omega}_M(x) &= \sum_{i}^{M} g_i(x)\eta_i = \sum_{i=1}^{M}\sum_{j=1}^{M}\sqrt{\lambda_j}q_{ij}f_j(x)\eta_i \\ &= \sum_{j=1}^{M}\sqrt{\lambda_j}f_j(x)\sum_{i=1}^{M}q_{ij}\eta_i = \sum_{j=1}^{M}\sqrt{\lambda_j}f_j(x)\xi_j\end{aligned} \tag{82}$$

where variable $\xi_j$ is defined by $\xi_j = \sum_{i=1}^{M} q_{ij}\eta_i$. Further, by virtue of the orthogonality property of $\mathbf{Q}$, we readily have $\sum_{i=1}^{M} q_{ij}q_{ik} = \delta_{jk}, (k, j = 1, 2, \cdots, M)$. Then, with the aid of this relation and the orthogonality of random variables $\eta_i$ leads to

$$\mathbb{E}\left[\xi_j\right] = \mathbb{E}\left[\sum_{i=1}^{M} q_{ij}\eta_i\right] = 0 \tag{83}$$

$$\begin{aligned}\mathbb{E}\left[\xi_j\xi_k\right] &= \mathbb{E}\left[\sum_{i=1}^{M} q_{ij}\eta_i \sum_{l=1}^{M} q_{lk}\eta_l\right] = \sum_{i=1}^{M}\sum_{l=1}^{M} q_{lk}q_{ij}\mathbb{E}\left[\eta_i\eta_l\right] \\ &= \sum_{i=1}^{M}\sum_{l=1}^{M} q_{lk}q_{ij}\delta_{il} = \sum_{i=1}^{M} q_{ik}q_{ij} = \delta_{kj}\end{aligned} \tag{84}$$

illustrating that random variable $\xi_j$ has zero mean and unit variance. Consequently, the covariance function corresponding to the truncated series in Eq.(82) becomes

$$\begin{aligned}\hat{C}(x_1, x_2) &= \sum_{i=1}^{M}\sum_{j=1}^{M}\sqrt{\lambda_j}q_{ij}f_j(x_1)\sum_{k=1}^{M}\sqrt{\lambda_k}q_{ik}f_k(x_2) = \sum_{j=1}^{M}\sum_{k=1}^{M}\sqrt{\lambda_j}\sqrt{\lambda_k}f_j(x_1)f_k(x_2)\sum_{i=1}^{M}q_{ij}q_{ik} \\ &= \sum_{j=1}^{M}\sum_{k=1}^{M}\sqrt{\lambda_j}\sqrt{\lambda_k}f_j(x_1)f_k(x_2)\delta_{jk} = \sum_{j=1}^{M}\lambda_j f_j(x_1)f_j(x_2)\end{aligned} \tag{85}$$

By comparing the truncated series representation in Eq.(82) and the resulting covariance function as derived in Eq.(85) with those in KL expansion, the convergence of the presented stochastic expansion directly follows from the Mercer theorem [31]. By the property $\mathbb{E}\left[\left(\omega(x) - \hat{\omega}_M(x)\right)^2\right] \to 0$, the truncation error can be made as small as desired. □

# References


[1] Roger G Ghanem and Pol D Spanos. *Stochastic finite elements: a spectral approach*. Dover Publications, INC, 2003.

[2] Peng Hao, Shaojun Feng, Hao Liu, Yutian Wang, Bo Wang, and Bin Wang. A novel Nested Stochastic Kriging model for response noise quantification and reliability analysis. *Computer Methods in Applied Mechanics and Engineering*, 384:113941, 2021.

[3] Guohai Chen and Dixiong Yang. Direct probability integral method for stochastic response analysis of static and dynamic structural systems. *Computer Methods in Applied Mechanics and Engineering*, 357:112612, 2019.

[4] Hongzhe Dai, Zhibao Zheng, and Huihuan Ma. An explicit method for simulating non-Gaussian and non-stationary stochastic processes by Karhunen-Loeve and polynomial chaos expansion. *Mechanical Systems and Signal Processing*, 115:1–13, 2019.

[5] Zhibao Zheng and Hongzhe Dai. A new fractional equivalent linearization method for nonlinear stochastic dynamic analysis. *Nonlinear Dynamics*, 91(2):1075–1084, 2018.

[6] Liam Comerford, Ioannis A Kougioumtzoglou, and Michael Beer. Compressive sensing based stochastic process power spectrum estimation subject to missing data. *Probabilistic Engineering Mechanics*, 44:66–76, 2016.

[7] Zhibao Zheng and Hongzhe Dai. Simulation of multi-dimensional random fields by Karhunen-Loeve expansion. *Computer Methods in Applied Mechanics and Engineering*, 324:221–247, 2017.

[8] Jun Xu and De Cheng Feng. Stochastic dynamic response analysis and reliability assessment of non-linear structures under fully non-stationary ground motions. *Structural Safety*, 79:94–106, 2019.

[9] Haihe Li, Pan Wang, Xiaoyu Huang, Zheng Zhang, Changcong Zhou, and Zhufeng Yue. Vine copula-based parametric sensitivity analysis of failure probability-based importance measure in the presence of multidimensional dependencies. *Reliability Engineering & System Safety*, 215:107898, 2021.

[10] Zhangjun Liu and Zenghui Liu. Random function representation of stationary stochastic vector processes for probability density evolution analysis of wind-induced structures. *Mechanical Systems and Signal Processing*, 106:511–525, 2018.

[11] M.D. Shields and G. Deodatis. A simple and efficient methodology to approximate a general non-Gaussian stationary stochastic vector process by a translation process with applications in wind velocity simulation. *Probabilistic Engineering Mechanics*, 31:19–29, 2013.

[12] Christian Soize and Roger G. Ghanem. Reduced chaos decomposition with random coefficients of vector-valued random variables and random fields. *Computer Methods in Applied Mechanics and Engineering*, 198(21):1926–1934, 2009.

[13] George Stefanou. The stochastic finite element method: Past, present and future. *Computer Methods in Applied Mechanics and Engineering*, 198(9-12):1031–1051, February 2009.

[14] Masanobu Shinozuka and C-M Jan. Digital simulation of random processes and its applications. *Journal of Sound and Vibration*, 25(1):111–128, 1972.

[15] Yongxin Wu, Yufeng Gao, Ning Zhang, and Fei Zhang. Simulation of spatially varying non-Gaussian and nonstationary seismic ground motions by the spectral representation method. *Journal of Engineering Mechanics, ASCE*, 144(1):04017143, 2018.

[16] Yongxin Wu and Yufeng Gao. A modified spectral representation method to simulate non-Gaussian random vector process considering wave-passage effect. *Engineering Structures*, 201:109587, 2019.

[17] Zhangjun Liu, Chenggao He, Zixin Liu, and Hailin Lu. Dimension reduction model for two-spatial dimensional stochastic wind field: Hybrid approach of spectral decomposition and wavenumber spectral representation. *Probabilistic Engineering Mechanics*, 60:103052, 2020.

[18] L. B. Li, K. K. Phoon, and S. T. Quek. Comparison between Karhunen-Loeve expansion and translation-based simulation of non-Gaussian processes. *Computers & Structures*, 85(5ĺC6):264–276, 2007.

[19] K.K. Phoon, S.P. Huang, and S.T. Quek. Simulation of second-order processes using Karhunen–Loeve expansion. *Computers & Structures*, 80(12):1049–1060, May 2002.

[20] K.K. Phoon, H.W. Huang, and S.T. Quek. Simulation of strongly non-Gaussian processes using Karhunen–Loeve expansion. *Probabilistic Engineering Mechanics*, 20(2):188–198, April 2005.

[21] Miroslav Vořechovsky. Simulation of simply cross correlated random fields by series expansion methods. *Structural safety*, 30(4):337–363, 2008.

[22] Heyrim Cho, D Venturi, and GE Karniadakis. Karhunen-loeve expansion for multi-correlated stochastic processes. *Probabilistic Engineering Mechanics*, 34:157–167, 2013.

[23] Dai Hongzhe, Zhibao Zheng, and Wei Wang. Nonlinear system stochastic response determination via fractional equivalent linearization and Karhunen–Loeve expansion. *Communications in Nonlinear Science and Numerical Simulation*, 49: 145-158, 2017.

[24] Wang, Mingzhi, Xu Yang, and Wei Wang. Establishing a 3D aggregates database from X-ray CT scans of bulk concrete. *Construction and Building Materials*, 315: 125740, 2022.

[25] Wolfgang Betz, Iason Papaioannou, and Daniel Straub. Numerical methods for the discretization of random fields by means of the Karhunen-Loeve expansion. *Computer Methods in Applied Mechanics and Engineering*, 271:109–129, April 2014.

[26] Diego Lorenzo Allaix and Vincenzo Ilario Carbone. Karhunen–Loeve decomposition of random fields based on a hierarchical matrix approach. *International Journal for Numerical Methods in Engineering*, 94(11):1015–1036, 2013.

[27] Xufang Zhang, Qian Liu, and He Huang. Numerical simulation of random fields with a high-order polynomial based Ritz–Galerkin approach. *Probabilistic Engineering Mechanics*, 55:17–27, 2019.

[28] Diego Lorenzo Allaix and Vincenzo Ilario Carbone. Development of a numerical tool for random field discretization. *Advances in Engineering Software*, 51:10–19, 2012.

[29] Pol D. Spanos, Michael Beer, and John Red-Horse. Karhunen-Loeve expansion of stochastic processes with a modified exponential covariance kernel. *Journal of Engineering Mechanics, ASCE*, 133(7):773–779, 2007.

[30] Zerva, Aspasia. *Spatial variation of seismic ground motions: modeling and engineering applications*. CRC Press, 2016.

[31] Hernandez D.B. *Lectures on probability and second-order random fields.* World Scientific, London, 1995.